

A STUDY ON OPTIMAL AND SLIDING MODE
GUIDANCE FOR AN INTERCEPTION
PROBLEM

By

JAE HONG SEO
Bachelor of Science
Inha University
Inchon, Korea
1996

Submitted to the Faculty of the
Graduate College of the
Oklahoma State University
in partial fulfillment of
the requirements for
the Degree of
MASTER OF SCIENCE
December, 2000

COPYRIGHT

By

JAE HONG SEO

December, 2000

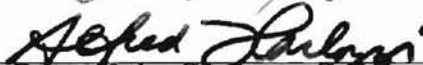
A STUDY ON OPTIMAL AND SLIDING MODE
GUIDANCE FOR AN INTERCEPTION
PROBLEM

Thesis Approved:


Thesis Adviser






Dean of the Graduate College

PREFACE

It is estimated that conventional missile guidance laws may not provide suitable performance for high maneuverable targets, and fundamental improvements in guidance logic may be necessary. Modern control methodology is believed to provide more systematic approach for the improvements.

In missile guidance, practical and academical interest is more of the guidance for the interception of high maneuvering target in space. As a control logic may has its own strong feature for a specific type of system, investigating a control logic which is best fit to guidance problem is another interest.

This paper suggests guidance laws derived from optimal control and sliding mode control, and compares them with conventional proportional navigation guidance for the target maneuvering in space. Performance of each guidance law is investigated via numerical simulation.

I wish to express my gratitude to my graduate advisor, Dr. Eduardo Misawa, for his invaluable support and advise in completion of this research. And I would like to thank to my graduate committee members, Dr. Arena and Dr. Pagilla for their guidance. I also thank to library and interlibrary service personnel for providing materials that were important to progress this research. Another thank is due to Dr. Brian O'Dell in MAE department for his help in preparing this paper using \LaTeX program. Finally I acknowledge my family who have always encouraged my successful academic achievement.

TABLE OF CONTENTS

1	Introduction	1
1.1	Introduction	1
1.2	Literature Rievew	2
1.3	Objective and Contribution of This Research	4
2	Guidance Law Design	6
2.1	Objective of Terminal Homing Guidance	6
2.2	Engagement Geometry	8
2.3	Proportional Navigation Guidance	11
2.3.1	Brief Review of Proportional Navigation Guidance	11
2.3.2	3D Proportional Navigation Guidance Law	12
2.4	Optimal Guidance Law	12
2.4.1	Brief Review of Optimal Control Problem	12
2.4.2	Time-optimal Guidance Law	14
2.4.3	Control-effort-optimal Guidance	20
2.4.4	A Note on the Derivation of \dot{p}_4, \dot{p}_5	23
2.4.5	Derivation of \dot{x} from Range and Angle Information	24
2.5	Sliding Mode Guidance Law	25
2.5.1	Brief Review of Sliding Mode Control Problem	25
2.5.2	Sliding Mode Guidance Law Design	27
3	Simulation and Analysis	33
3.1	Simulation and Analysis	33

3.2	2D Simulation and Analysis	35
3.2.1	Notable Characteristics of Optimal and Sliding Mode Guidance	35
3.2.2	Comparison of Guidance Laws	49
3.3	3D Simulation Results	57
4	Conclusion	64
	Bibliography	66
A	Simulation Program	70

LIST OF TABLES

3.1	Miss distance caused by t_{go} and x_f estimation error	41
3.2	Comparison of guidance laws in miss distance and time	51
3.3	Summary of statistical miss distance	63

LIST OF FIGURES

2.1	Missile flight profile [15]	6
2.2	Typical proximity fuze pattern [15]	7
2.3	Engagement Geometry : (a) 3-D Engagement geometry (b) Geometry projected on θ -plane (c) γ_m -plane (d) Geometry projected on ϕ -plane (ψ_m -plane)	10
2.4	Collision triangle	11
3.1	TOG for ideal case: (a) Missile-target engagement (b) Acceleration (c) Missile flight path angle (d) Estimated final states (e) Enlargement of (d)	37
3.2	TOG with final states estimation filter (filter time constant 0.2 sec.) : (a) Missile-target engagement (b) Acceleration (c) Missile flight path angle (d) Estimated final states	38
3.3	TOG with response delay (time constant 0.2 sec.) : (a) Missile-target engagement (b) Acceleration (c) Missile flight path angle (d) Estimated final states	39
3.4	TOG with missile dynamics time constant 0.2 sec.: (a) Acceleration (b) Estimated final states	40
3.5	TOG with missile dynamics time constant 0.5 sec. : (a) Acceleration (b) Estimated final states	40

3.6	COG for simple maneuvering target : (a) Missile-target engagement (b) Acceleration (c) Missile flight path angle (d) Estimated final states (e) Enlargement of (d)	42
3.7	COG with missile dynamics time constant 0.2 sec.: (a) Acceleration (b) Estimated final states	43
3.8	COG with missile dynamics time constant 0.5 sec.: (a) Acceleration (b) Estimated final states	43
3.9	COG with constant penalty coefficients : (a) Acceleration (b) Estimated final states	44
3.10	COG with time varying penalty coefficients : (a) Acceleration (b) Estimated final states	44
3.11	SMG for a simple target: (a) Missile-target engagement (b) Acceleration and control gain k (c) s function (LOS rate) (d) Missile flight path angle and LOS angle	46
3.12	Adaptation parameters and s	47
3.13	Control gain k without initial heading error (a) Acceleration (b) LOS rate (s)	48
3.14	Comparison of guidance laws for a non-maneuvering target : (a) Missile-target engagement (b) Acceleration (c) LOS rate (d) Missile flight path angle and LOS angle	53
3.15	Comparison of guidance laws for a simple 10g maneuvering target : (a) Missile-target engagement (b) Acceleration (c) LOS rate (d) Missile flight path angle and LOS angle	54
3.16	Comparison of guidance laws for a weaving target : (a) Missile-target engagement (b) Acceleration (c) LOS rate (d) Missile flight path angle and LOS angle	55

3.17	Miss distance to different target maneuver start time : (a) Missile-target engagement (b) Miss distance comparison	56
3.18	3D missile-target engagement : (a) Missile-target engagement (b) θ plane view (c) ϕ plane view	59
3.19	Statistical miss distance comparison 1: Initial distance (6000,1000,1000) (a) Miss distance (b) Missile acceleration usage (c) Elapsed time . . .	60
3.20	Statistical miss distance comparison 2: Initial distance (9000,3000,3000)	61
3.21	Statistical miss distance comparison 3: $v_m = 400m/s$ $v_t = 800m/s$, Initial distance (7000,0,0)	61
3.22	Statistical miss distance comparison 4: Initial distance (6000,1000,1000), range rate noise (0, 1000)	62
3.23	Statistical miss distance comparison 5: Initial distance (6000,1000,1000), LOS rate noise (0, 10^{-2})	62
3.24	An example of random target acceleration	63
A.1	PN Guidance Simulation Program	71
A.2	Optimal Guidance Simulation Program	72
A.3	Sliding Mode Guidance Simulation Program	73

Chapter 1

Introduction

1.1 Introduction

Guidance laws for short-range tactical missiles have been widely researched since the first appearance of the missile system approximately five decades ago. The earlier guidance laws, referred to as classical guidance, are line-of-sight (LOS), pursuit and proportional navigation guidance (PNG) [19]. Those LOS and pursuit guidance laws are observed to have limited capability to engage maneuvering targets, while the PNG has been widely used in terminal homing guidance in the virtue of its simplicity, easily attainable measurement, relatively easy implementation, and acceptable performance in various application fields such as surface-to-air and air-to-air missile systems including stationary targets and nonmaneuverable targets. This guidance scheme is still effective with current targets when missiles are superior to the targets in velocity and acceleration capability. However PNG performance is seriously degraded for high maneuvering targets.

A challenge in the tactical air-to-air missile guidance is in interception of highly maneuverable aircrafts. It is estimated that classical guidance laws are not adequate in the engagement with those high maneuverable advanced targets. Several other variants of proportional navigation have been invented in an effort to improve PNG,

requiring explicit knowledge of target and missile acceleration information. In addition the variants of PNG, so called modern guidance laws based on LQ optimal control theory have been intensively researched to enhance fundamental advances in the effectiveness of missile guidance technique. LQ optimal guidance has the capability of taking into account the cost and the time in the guidance law design as well as miss distance, yet it has its own difficulties in practical implementation such as requirements of accurate time-to-go estimation and target acceleration estimation. Very recently sliding-mode control theory has drawn attention of several researchers in the guidance law design.

1.2 Literature Rieview

Many literatures have dealt with various aspects of PNG. For the fundamentals of the proportional navigation, Murtaugh and Criel [18] explained the nature of basic theory of PNG and its variations in tutorial manner. Comprehensive aspects of proportional navigation including fundamental theory and additional important considerations associated with its practical application is provided in Zarchan [28].

Readable survey papers for guidance research history were provided by Pastrick et al. [19] and Cloutier et al. [7]. Pastrick et al. collected scattered guidance literature ranging from classical approach to early modern guidance technology that is applicable to short-range missiles. Cloutier et al. surveyed literature on modern air-to-air guidance technology including target state estimation and bank-to-turn autopilot. The earlier work for three-dimensional guidance is found in [1], which extended planar proportional navigation to three-dimension and, after linearizing the obtained equations, studied missile trajectories analytically to find the adequate range of the effective navigation ratio and the ratio of missile velocity to closing velocity for successful interception of targets. Kreindler [17] mathematically proved from linearized

planar engagement geometry that proportional navigation is, for a nonmaneuvering target with constant velocity, a type of LQ optimal guidance.

Salama and Hamza [20] analyzed the minimum-time interception trajectories for a fixed target in 3D space. Siouris and Leros [21] presented a tutorial for designing minimum-time interception trajectories based on time-optimal control, which was illustrated by an interception example for a nonmaneuvering target. Hartman et al. [11] designed time-optimal guidance under several practical constraints including LOS limitation and investigated the influence of the seeker measurement performance on optimal interception trajectories. In [12] time-optimal guidance logic was used to construct a time-to-go prediction algorithm other than simple range over closing velocity scheme, and applied the proposed algorithm to LQ guidance law to improve interception performance. Song and Shin [23] studied time-optimal guidance with impact angle control in vertical plane engagement and suggested a numerical algorithm via geometrical approach to determine optimal acceleration switching time.

The earliest literature of sliding-mode guidance is introduced by Brierley and Longchamp [5], where sliding mode control was applied for nonlinear two-dimensional interception problem with integrated guidance-autopilot model and showed the robustness of the proposed guidance law. Babu et al. [2] proposed a version of sliding-mode guidance law with an adaptation logic and qualitatively compared the suggested guidance laws with the PNG, and in [3] they extended their earlier work by applying sliding mode estimator to missile guidance problem. Benshabat and Bar-Gill [4] applied sliding mode to command-to-line-of-sight guidance for a sea-skimming missile with an integrated guidance-autopilot model and achieved a robust guidance algorithm. Zhou et al. [30] formalized the sufficient and necessary condition for the invariance of sliding mode for linear time varying system, and derived an adaptive sliding mode guidance based on the condition. Zhou et al. also proposed [29] a guidance scheme by integrating optimal control into sliding mode guidance in order to

combine strength of both control logic into one algorithm.

1.3 Objective and Contribution of This Research

Considerable research work have been devoted to terminal missile guidance laws. Modern guidance technology, based on LQ optimal control, provides systematic framework for the development of guidance within given criteria and missile performance limitations. LQ optimal guidance is based on linearized model and in some cases requires estimations of target states that may be difficult in practical implementations.

Little literature have dealt with time-optimal guidance. Most of the literature have focused on analytic solution of minimum-time missile trajectories. Those analytic approach inevitably adopted some types of simplification such as stationary or nonmaneuverable target and linearization. Though they provide good perspective of the guidance law, only limited analysis is possible. In addition, all the reported time-optimal guidance laws were developed with a fixed final states of boundary conditions whose typical solver would involve iteration of forward integration of the states equation and backward integration of the costate equation until the solution converge [6], and are limited by the requirements of high computational efforts in finding the optimum control law.

Sliding mode control, a well known robust control methodology, have recently applied guidance problem in several literature and demonstrated the prospect of sliding mode guidance law. Sliding mode guidance is relatively young and requires more investigation for various engagement model as well as 3D interception which is not reported yet.

The objective of this research is to construct guidance law based on optimal control and sliding mode control considering three dimensional full nonlinear engagement model, and compare them with PNG in the characteristic and interception perfor-

mance for high maneuverable targets via numerical simulations. For the purpose, 3D sliding mode guidance, optimal guidance and proportional guidance were developed and investigated via numerical simulation. In the development of time-optimal guidance, unlike existing literature, 'free final state' approach is selected, which requires less computation effort and is of more practical in a sense. Sliding mode guidance is structured based on basic guidance strategy of proportional navigation. An adaptation logic is proposed to determine the sliding mode control gain.

Chapter 2

Guidance Law Design

2.1 Objective of Terminal Homing Guidance

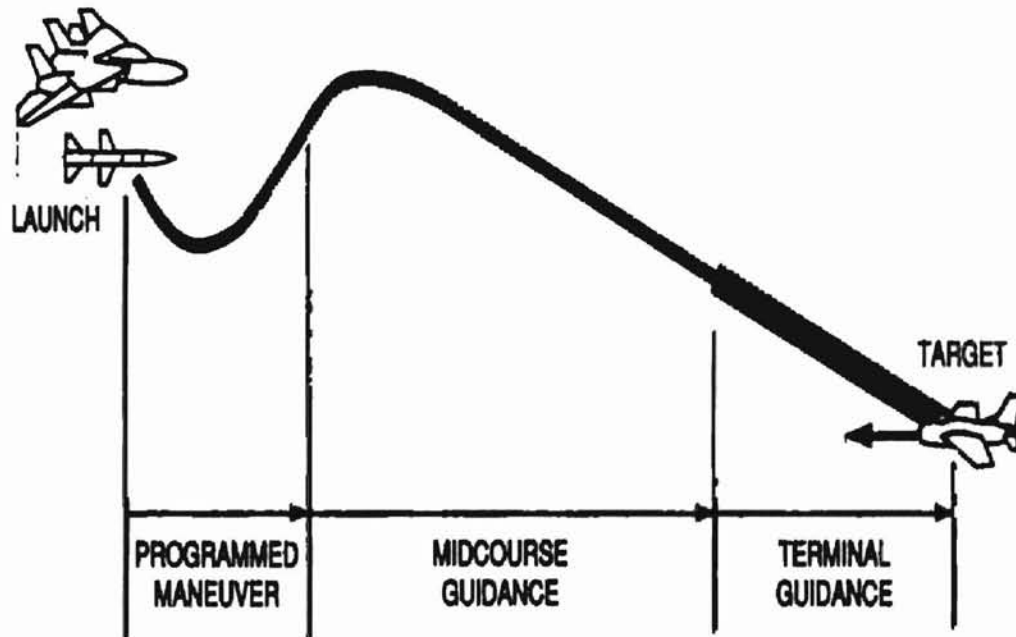


Figure 2.1: Missile flight profile [15]

The guidance stage of a tactical missile is commonly divided into three phases: launch, mid-course, and terminal homing phase. After a missile is launched, mid-course guidance places the missile within the range where the missile seeker acquires

target, during which estimation of target position and velocity is provided by the launch aircraft or other ground platforms. The terminal homing guidance is from the seeker acquisition of the target to interception, where terminal acquisition parameters such as LOS angle, range, and range rate (with Doppler radar) are provided by the missile seeker.

Besides the seeker, tactical missiles are usually incorporated with another sensor called proximity fuzes [15] as shown in Figure 2.2. The proximity fuze detects the target when missile closes, and detonates the missile without physical contact with the target, which is to increase the interception probability.

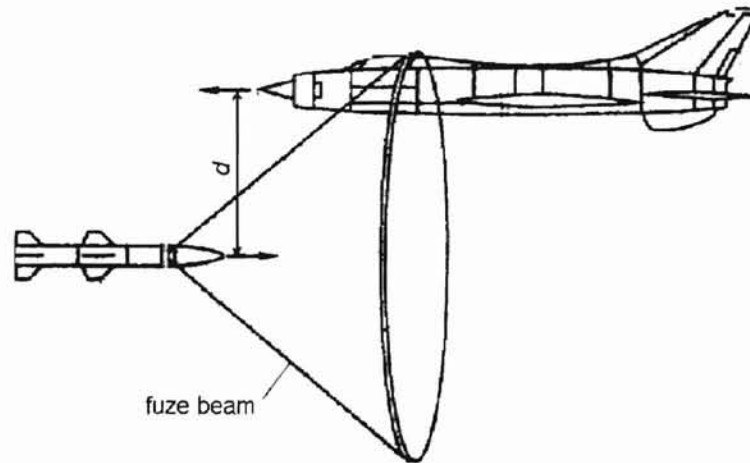


Figure 2.2: Typical proximity fuze pattern [15]

When the missile crosses the target without interception, then the missile may be expected to turn around and follow the target, but that is the highly undesirable situation. Missiles are operated with the limited amount of fuel which signifies the operation time in missile guidance, and hence missiles are expected to intercept targets in the possible shortest time. Once the missile fails to intercept when it crosses the target for the first time, then the missile would not intercept the same maneuvering target again even if it would make turn around and engage again, which means the missile would never intercept the target. Most of all, as there may exist practical

limitation of seeker acquisition range in angle, once the missile crosses the target, the seeker limitation may make the seeker not to be able to detect the target behind of the missile, and the homing guidance can not be effective any longer. Therefore, after the missile is launched, the instant when the missile passes the target for the first time is considered as the final stage of missile guidance, and the ultimate objective of the terminal guidance is, at that instant, to decrease missile-target relative distance d (Figure 2.2) into within the fuze detectable range, or more desirably to zero.

2.2 Engagement Geometry

Short range tactical homing missile is considered. This research is about missile trajectory shaping for the interception of targets, and thus missile dynamics are neglected except for response delay. Additionally considering short range of missile operation, the following assumptions are made in the guidance law design;

1. the earth is flat,
2. missile and target are point masses,
3. both gravitational and drag force are negligible,
4. velocities of missile and target remain constant,
5. missile is completely roll-stabilized so that pitch and yaw motions are decoupled and controlled separately, and
6. all missile states are measurable.

Either Cartesian or spherical coordinate system can be used to describe missile-target engagement geometry. As seeker measurements are range and range angles which consist of spherical coordinate system [28], Cartesian system requires a transformation of the measurements. In this paper, PNG and sliding mode guidance will be synthesized from spherical coordinate system while optimal guidance will be derived based on Cartesian system with a transformation from spherical to Cartesian.

The point mass missile-target engagement geometry in spherical coordinate system with the missile being the origin is depicted in Figure 2.3(a). Figure 2.3(b), (c) and (d) show planar engagement geometry projected in each θ plane¹, γ_m plane and $\phi(\psi)$ plane respectively.

< Nomenclature for Figure 2.3 >

(1,2,3)	Missile body coordinate system, moving but non-rotating w.r.t. inertial frame
M (T)	Missile(target) position
r (r')	Relative distance between missile and target (projected on ϕ plane) : LOS
θ, ϕ	Azimuth angles of r ; LOS angles
γ_m	Missile pitch angle
ψ_m	Missile yaw angle
$\gamma_{m/\theta}$	γ_m projected on θ plane
v_m	Missile velocity vector in space
$v_{m/\theta}$	v_m projected on θ plane
$v_{m\theta}$	θ -component of v_m
v_{mr}	r -component of v_m
$v_{m\phi}$	A component of v_m in ϕ direction
v_{m1}, v_{m2}, v_{m3}	Axes 1,2,3-component of v_m respectively
$a_{m\theta}$	Missile acceleration perpendicular to r in θ plane
$a_{m\phi}$	Missile acceleration perpendicular to r' in ϕ plane
$n_\theta (= n_\gamma)$	Missile acceleration perpendicular to $v_{m/\theta}$ in θ plane (= Pitch-directional missile acceleration)
$n_\phi (= n_\psi)$	Missile acceleration perpendicular to $v_m \cos \gamma_m$ in ϕ plane (= Yaw-directional missile acceleration)

Note

1. $n_\theta = n_\gamma$ and $n_\phi = n_\psi$: Clearly $n_\phi = n_\psi$ as angles ϕ and ψ are defined in the same plane. n_θ is normal to the plane composed of $Mv_m v_{m/\theta}$, and hence also normal to v_m in γ plane.
2. These notations are same for the target with subscript m replaced by t

¹ θ plane: plane where angle θ lies. γ_m plane, ϕ plane and ψ plane are defined in the same way. This notation will be used throughout this paper. ϕ and ψ are on the same plane but different name will be used to maintain clear notation in the derivation of guidance laws.

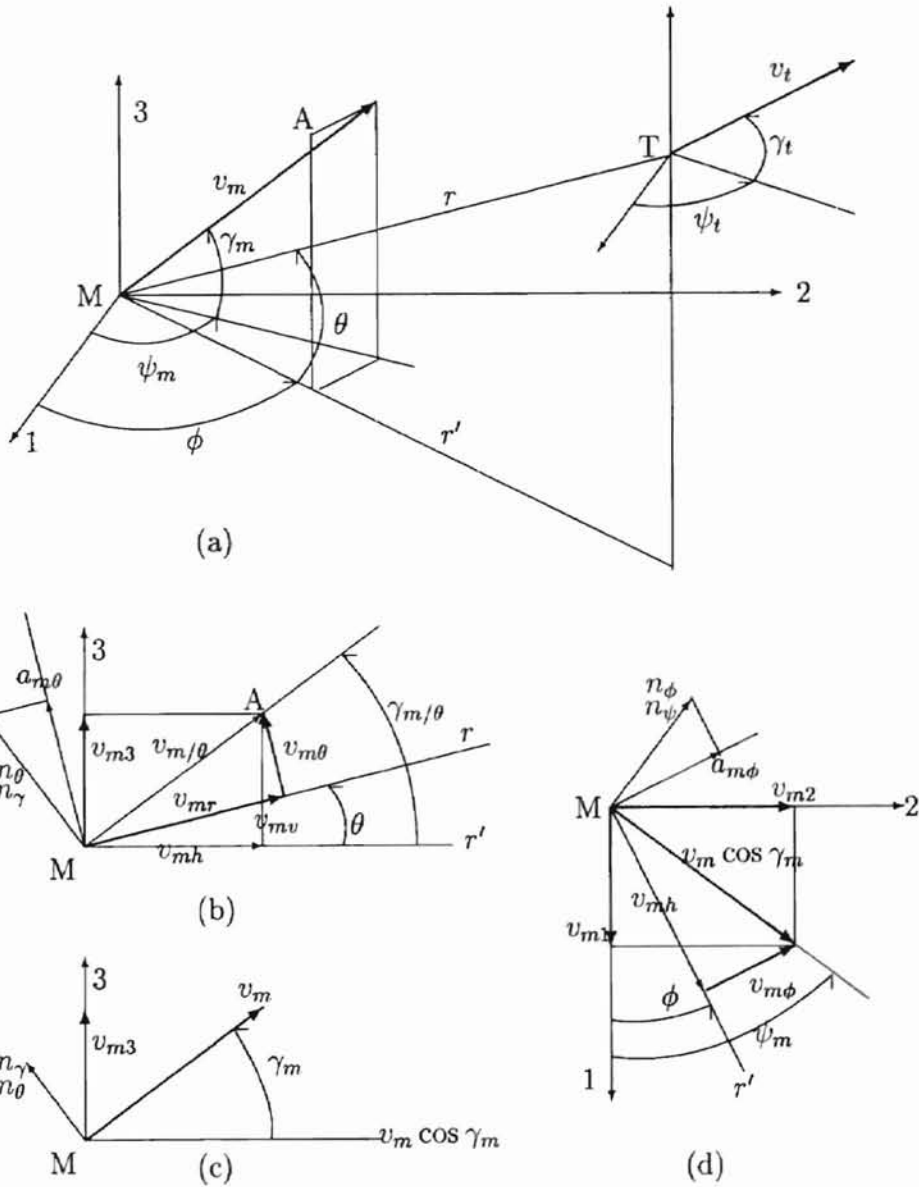


Figure 2.3: Engagement Geometry : (a) 3-D Engagement geometry (b) Geometry projected on θ plane (c) γ_m plane (d) Geometry projected on ϕ plane (ψ_m plane)

2.3 Proportional Navigation Guidance

2.3.1 Brief Review of Proportional Navigation Guidance

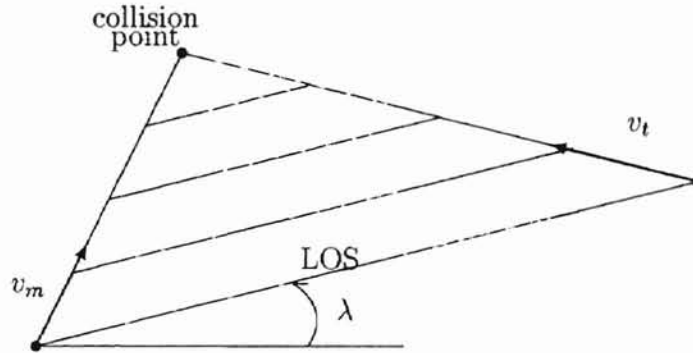


Figure 2.4: Collision triangle

The basic idea of the proportional navigation is simple. Consider Figure 2.4, where LOS is the imaginary line connecting missile and target, λ is LOS angle measured from inertial reference. Assume v_m and v_t are constant and target is non-maneuvering. If the rotation rate of LOS angle is kept zero, or the LOS angle remains constant, then missile and target will establish the collision triangle and eventually collide at the 'collision point'. This is intuitively true even if target would maneuver, and has been proven through vector analysis [15]. A missile flying in the way that the collision triangle is satisfied will travel along a straight line that is clearly the least distance for the interception of the target. The straight line requires the minimum time and control effort from the missile, and hence consists of an optimum missile trajectory.

PNG is to zero LOS rate by issuing missile acceleration command normal to instantaneous LOS so as to hold LOS angle constant. The PNG is formalized as

$$n_c = NV_c \dot{\lambda} \quad [\text{rad} \cdot \text{m}/\text{s}^2] \quad (2.1)$$

where n_c is acceleration command, N is control gain known as *effective navigation*

ratio, V_c is missile-target closing velocity and $\dot{\lambda}$ is the time derivative of the LOS angle or the LOS rate. N commonly ranges between 3–5, which means the missile will turn faster than LOS.

2.3.2 3D Proportional Navigation Guidance Law

Consider Figure 2.3. LOS are composed of two angles defined as θ and ϕ . Following the given assumption that missile pitch and yaw motion are decoupled, separated missile acceleration command in each θ plane and ϕ plane is considered. Range r and its projection to ϕ plane $r' = r \cos \theta$ are the missile-target relative distance in θ plane and in ϕ plane respectively. Then the closing velocity in each plane can be stated as $-\dot{r}$ and $-(\dot{r} \cos \theta - r\dot{\theta} \sin \theta)$. Extension of (2.1) to this three-dimensional leads the acceleration command normal to each angle θ and ϕ to be

$$\begin{aligned} n_{c\theta} &= -N\dot{r}\dot{\theta} \\ n_{c\phi} &= -N(\dot{r} \cos \theta - r\dot{\theta} \sin \theta)\dot{\phi}. \end{aligned}$$

And from the relation $v_{m/\theta} \sin \gamma_{m/\theta} = v_m \sin \gamma_m$ in Figure 2.3(a)(b), $\gamma_{m/\theta}$ is derived as

$$\gamma_{m/\theta} = \sin^{-1} \left(\frac{v_m \sin \gamma_m}{v_{m/\theta}} \right) = \sin^{-1} \left(\frac{v_m \sin \gamma_m}{\sqrt{v_m^2 - v_{m\phi}^2}} \right). \quad (2.2)$$

Then the missile acceleration command normal to LOS angles can be expressed as

$$\begin{aligned} n_\theta &= \frac{-N\dot{r}\dot{\theta}}{\cos(\gamma_{m/\theta} - \theta)} \\ n_\phi &= \frac{-N(\dot{r} \cos \theta - r\dot{\theta} \sin \theta)\dot{\phi}}{\cos(\psi_m - \phi)}. \end{aligned}$$

2.4 Optimal Guidance Law

2.4.1 Brief Review of Optimal Control Problem

A brief review of optimal control problem is presented in this section.

For a system presented by

$$\dot{\mathbf{x}}(t) = \mathbf{f}(\mathbf{x}(t), \mathbf{u}(t), t) \quad (2.3)$$

where $\mathbf{x}(t) \in R^n$ is the state, $\mathbf{u}(t) \in R^m$ is the control. The optimal control problem is to find a control $\mathbf{u}^* \in \mathbf{U}$ which controls the system (2.3) to follow a trajectory $\mathbf{x}^* \in \mathbf{X}$ such that minimizes the *performance index*

$$\mathbf{J} = h(\mathbf{x}(t_f), t_f) + \int_{t_0}^{t_f} g(\mathbf{x}(t), \mathbf{u}(t), t) dt \quad (2.4)$$

where \mathbf{u}^* is called an optimal control and \mathbf{x}^* an optimal trajectory, \mathbf{U} and \mathbf{X} denotes all admissible control and all admissible trajectory respectively, $h(\cdot)$ is weighted final states, $g(\cdot)$ is parameters to be minimized, and t_f stands for final time and t_0 initial time.

Selection of the performance index depends on parameters which when minimized the system performs in the most desirable manner for a particular problem. Once the performance index is chosen, the next step is to determine a control function that minimizes this criterion. Two methods in the minimization are the *Dynamic programming* method and the *Variational* approach which leads to, in most cases, a nonlinear two-point boundary-value problem. The *Pontryagin's minimum principle* is an extension of the variational approach taking account for the effects of control restraints. Conditions required to develop optimal control is summarized below.

For the system (2.3) and the performance index (2.4), the *Hamiltonian* is defined as

$$H(\mathbf{x}(t), \mathbf{u}(t), \mathbf{p}(t), t) = g(\mathbf{x}(t), \mathbf{u}(t), t) + \mathbf{p}^T[\mathbf{f}(\mathbf{x}(t), \mathbf{u}(t), t)] \quad (2.5)$$

where \mathbf{p} is called costate whose value is to be determined. According to Pontryagin's minimum principle, the necessary conditions for $\mathbf{u}(t)$ to be an optimal control [16] are

$$\dot{\mathbf{x}}^*(t) = \frac{\partial H}{\partial \mathbf{p}}(\mathbf{x}^*(t), \mathbf{u}^*(t), \mathbf{p}^*, t) \quad (2.6)$$

$$\dot{\mathbf{p}}^*(t) = -\frac{\partial H}{\partial \mathbf{x}}(\mathbf{x}^*(t), \mathbf{u}^*(t), \mathbf{p}^*, t) \quad (2.7)$$

$$H(\mathbf{x}^*(t), \mathbf{u}^*(t), \mathbf{p}^*(t), t) \leq H(\mathbf{x}^*(t), \mathbf{u}(t), \mathbf{p}^*(t), t) \quad (2.8)$$

where $\dot{\mathbf{x}}^*(t)$ is the state equation and $\dot{\mathbf{p}}^*(t)$ is called costate equation. And boundary conditions are given to be

$$\left[\frac{\partial h}{\partial \mathbf{x}}(\mathbf{x}^*(t_f), t_f) - \mathbf{p}^*(t_f) \right]^T \delta \mathbf{x}_f + \left[H(\mathbf{x}^*(t_f), \mathbf{u}^*(t_f), \mathbf{p}^*(t_f), t_f) + \frac{\partial h}{\partial t}(\mathbf{x}^*(t_f), t_f) \right] \delta t_f = 0. \quad (2.9)$$

The boundary conditions are determined by making appropriate substitutions in (2.9) according to the problem formulated. For the problems with free final states and free final time, $\delta \mathbf{x}_f$ and δt_f are arbitrary and hence their coefficients must be zero, which yields boundary conditions given by

$$\mathbf{p}^*(t_f) = \frac{\partial h}{\partial \mathbf{x}}(\mathbf{x}^*(t_f), t_f) \quad (2.10)$$

$$H(\mathbf{x}^*(t_f), \mathbf{u}^*(t_f), \mathbf{p}^*(t_f), t_f) + \frac{\partial h}{\partial t}(\mathbf{x}^*(t_f), t_f) = 0. \quad (2.11)$$

2.4.2 Time-optimal Guidance Law

The objective of the time-optimal guidance is to transfer a missile from an arbitrary initial position to a target position in minimum time. The guidance strategy considered in this paper is to zero relative distance between missile and target, which will eventually bring the missile to the position of target. As the interesting parameter is the elapsed time for interception, maximum control effort is set to be used throughout the operation, which will form the *bang-bang control*. As it is assumed that missile pitch and yaw motion is decoupled, separated guidance in each motion is considered. Derivation of a time-optimal control for this problem is presented below with '*' and arguments except t_f (final time) omitted for simplicity unless it causes confusion.

Time-optimal Guidance for Ideal Model

Consider Figure 2.3. Let v_{tp} and v_{mp} be target and missile velocity components in ϕ plane;

$$v_{tp} = v_t \cos \gamma_t, \quad v_{mp} = v_m \cos \gamma_m.$$

Choose the states to be relative distance on each reference axis x_1, x_2, x_3 , missile flight path angle γ_m and yaw angle ψ_m ($[x_1 \ x_2 \ x_3 \ \gamma_m \ \psi_m]$). The equations of motion are given by

$$\begin{aligned} \dot{x}_1 &= v_{t1} - v_{m1} = v_{tp} \cos \psi_t - v_{mp} \cos x_5 \\ \dot{x}_2 &= v_{t2} - v_{m2} = v_{tp} \sin \psi_t - v_{mp} \sin x_5 \\ \dot{x}_3 &= v_{t3} - v_{m3} = v_t \sin \gamma_t - v_m \sin x_4 \\ \dot{x}_4 &= \dot{\gamma}_m = \frac{n_\gamma}{v_m} = \frac{n_{max}}{v_m} u_\gamma \\ \dot{x}_5 &= \dot{\psi}_m = \frac{n_\psi}{v_{mp}} = \frac{n_{max}}{v_{mp}} u_\psi \end{aligned} \quad (2.12)$$

where n_{max} is maximum admissible control, u_γ and u_ψ are units whose signs are to be determined. Considering time as the parameter to be minimized, the performance index with weighted final states is

$$J = \frac{1}{2} (x_1^2(t_f) + x_2^2(t_f) + x_3^2(t_f)) + \int_{t_0}^{t_f} dt. \quad (2.13)$$

The Hamiltonian is

$$\begin{aligned} H &= 1 + p_1(v_{tp} \cos \psi_t - v_{mp} \cos x_5) \\ &\quad + p_2(v_{tp} \sin \psi_t - v_{mp} \sin x_5) \\ &\quad + p_3(v_t \sin \gamma_t - v_m \sin x_4) \\ &\quad + p_4 \left(\frac{n_{max}}{v_m} u_\gamma \right) + p_5 \left(\frac{n_{max}}{v_{mp}} u_\psi \right). \end{aligned} \quad (2.14)$$

According to Pontryagin's Minimum principle, the necessary conditions for an optimal control is

$$p_4 \frac{n_{max}}{v_m} u_\gamma^* \leq p_4 \frac{n_{max}}{v_m} u_\gamma$$

$$p_5 \frac{n_{max}}{v_{mp}} u_\psi^* \leq p_5 \frac{n_{max}}{v_{mp}} u_\psi \quad (2.15)$$

which determines the control to be

$$\begin{aligned} u_\gamma^* &= -sgn(p_4) \\ &= \text{undefined for } p_4 = 0 \\ u_\psi^* &= -sgn\left(\frac{p_5}{v_{mp}}\right), v_{mp} \neq 0 \\ &= \text{undefined for } p_5 = 0 \end{aligned} \quad (2.16)$$

where $sgn(\cdot)$ is usual signum function whose value is defined as +1 when (\cdot) is positive and -1 when negative. When $p_4 = 0$ and $p_5 = 0$ control law u_γ^* and u_ψ^* are not defined from the relation (2.15), which is called *singular condition*. At the isolated singular points control switches between \pm and this discontinuous control forms well-known bang-bang operation. When the singular condition exists in some finite time interval, it is referred as *singular interval*.

Equation (2.16) shows that the required parameters to generate the control are p_4 and p_5 , which can be derived from the costate equations and given boundary conditions. The costate equations are

$$\dot{p}_1 = -\frac{\partial H}{\partial x_1} = 0 \quad (2.17)$$

$$\dot{p}_2 = -\frac{\partial H}{\partial x_2} = 0 \quad (2.18)$$

$$\dot{p}_3 = -\frac{\partial H}{\partial x_3} = 0 \quad (2.19)$$

$$\dot{p}_4 = -\frac{\partial H}{\partial x_4} = p_3 v_m \cos x_4 \quad (2.20)$$

$$\dot{p}_5 = -\frac{\partial H}{\partial x_5} = -v_{mp}(p_1 \sin x_5 - p_2 \cos x_5). \quad (2.21)$$

From the boundary conditions of free final states and free final time,

$$p_1(t_f) = x_1(t_f) \quad (2.22)$$

$$p_2(t_f) = x_2(t_f) \quad (2.23)$$

$$p_3(t_f) = x_3(t_f) \quad (2.24)$$

$$p_4(t_f) = 0 \quad (2.25)$$

$$p_5(t_f) = 0. \quad (2.26)$$

(2.17)-(2.19) implies p_1, p_2, p_3 are constants with respect to time, and hence with (2.22)-(2.24) it can be concluded that

$$p_1 = p_1(t_f) = x_1(t_f) \quad (2.27)$$

$$p_2 = p_2(t_f) = x_2(t_f) \quad (2.28)$$

$$p_3 = p_3(t_f) = x_3(t_f). \quad (2.29)$$

Integral of (2.20)(2.21) yields

$$\int_{t_0}^{t_f} \dot{p}_4 dt = p_4(t_f) - p_4(t) = p_3 v_m \cos x_4 (t_f - t_0) \quad (2.30)$$

$$\int_{t_0}^{t_f} \dot{p}_5 dt = p_5(t_f) - p_5(t) = -v_{mp}(p_1 \sin x_5 - p_2 \cos x_5)(t_f - t_0) \quad (2.31)$$

where t_0 is an arbitrary initial time, hence it can be replaced with the general notation t , then with (2.25)(2.26)

$$p_4 = -p_3 v_m \cos x_4 t_{go} \quad (2.32)$$

$$p_5 = v_{mp}(p_1 \sin x_5 - p_2 \cos x_5) t_{go} \quad (2.33)$$

where t_{go} is time-to-go for interception and can be obtained from range over range rate, which is

$$t_{go} = t_f - t = \frac{r}{-\dot{r}} = \frac{\text{relative distance}}{\text{closing velocity}}.$$

The simplest way to decide $x_1(t_f), x_2(t_f)$ and $x_3(t_f)$ may be

$$\begin{aligned} x_1(t_f) &= x_1(t) + \dot{x}_1 \cdot t_{go} \\ x_2(t_f) &= x_2(t) + \dot{x}_2 \cdot t_{go} \\ x_3(t_f) &= x_3(t) + \dot{x}_3 \cdot t_{go}. \end{aligned} \quad (2.34)$$

t_{go} and the final states (2.34) are the necessary parameters to generate control input (2.16) and to be estimated online through out the interception process. Then this optimal guidance is of two point boundary value problem: fixed initial points (given initial states are known) and free time varying final points.

For the singular condition in (2.16), interest is given in *singular interval* rather than isolated singular points. For the singular interval to exist, there must be a period of time when $p_4 = \dot{p}_4 = 0$ and $p_5 = \dot{p}_5 = 0$. If $\dot{p}_4 = 0$, in (2.20) p_3 should be zero because $v_m \cos x_4 = v_{mp}$ cannot be zero from the requirement in (2.16), which violates the condition of p_3 being constant. From (2.21) \dot{p}_5 is zero for a time interval only if $p_1 = p_2 = 0$ which violates the condition p_1 and p_2 are constants. In another point of view, if $p_1 = p_2 = p_3 = 0$ then $H = 1$ from (2.14). But the boundary condition $H(t_f) = 0$ in (2.11) means $H = 0$ because H is not a function of time explicitly. It conflicts. Therefore it can be concluded that no singular interval exist.

Time-optimal Guidance with Response Delay

Known and well formalized disturbances can be included in optimization. Assume the flight-control system dynamics were modeled as a single lag in both pitch and yaw motion, or

$$\frac{\bar{n}_\gamma}{n_\gamma} = \frac{1}{1 + sT}, \quad \frac{\bar{n}_\psi}{n_\psi} = \frac{1}{1 + sT} \quad (2.35)$$

where $\bar{n}_\gamma, \bar{n}_\psi$ are achieved missile acceleration, n_γ, n_ψ are commanded acceleration and T is time constant. Then state equation (2.12) should be modified to

$$\begin{aligned} \dot{x}_1 &= v_{tp} \cos \psi_t - v_{mp} \cos x_5 \\ \dot{x}_2 &= v_{tp} \sin \psi_t - v_{mp} \sin x_5 \\ \dot{x}_3 &= v_t \sin \gamma_t - v_m \sin x_4 \\ \dot{x}_4 &= \frac{\bar{n}_\gamma}{v_m} \\ \dot{x}_5 &= \frac{\bar{n}_\psi}{v_{mp}} \end{aligned}$$

$$\begin{aligned}\dot{\bar{n}}_\gamma &= \frac{n_{max}u_\gamma - \bar{n}_\gamma}{T} \\ \dot{\bar{n}}_\psi &= \frac{n_{max}u_\psi - \bar{n}_\psi}{T}.\end{aligned}$$

The Hamiltonian is

$$\begin{aligned}H(t) &= 1 + p_1(v_{tp} \cos \psi_t - v_{mp} \cos x_5) + p_2(v_{tp} \sin \psi_t - v_{mp} \sin x_5) \\ &+ p_3(v_t \sin \gamma_t - v_m \sin x_4) + p_4 \left(\frac{\bar{n}_\gamma}{v_m} \right) + p_5 \left(\frac{\bar{n}_\psi}{v_{mp}} \right) \\ &+ p_6 \left(\frac{n_{max}u_\gamma - \bar{n}_\gamma}{T} \right) + p_7 \left(\frac{n_{max}u_\psi - \bar{n}_\psi}{T} \right).\end{aligned}$$

From Pontryagin's minimum principle, requirements for the optimal control is

$$\begin{aligned}\frac{p_6 n_{max} u_\gamma^*}{T} &\leq \frac{p_6 n_{max} u_\gamma}{T} \\ \frac{p_7 n_{max} u_\psi^*}{T} &\leq \frac{p_7 n_{max} u_\psi}{T}\end{aligned}\quad (2.36)$$

which sets the control law to be

$$\begin{aligned}u_\gamma^* &= -\text{sgn}(p_6) \\ &= \text{undefined if } p_6 = 0 \\ u_\psi^* &= -\text{sgn}(p_7) \\ &= \text{undefined if } p_7 = 0.\end{aligned}\quad (2.37)$$

From costate equation (2.7), p_1 - p_5 are same as (2.27)-(2.29)(2.32)(2.33) but

$$\begin{aligned}\dot{p}_6 &= -\left(\frac{p_4}{v_m} - \frac{p_6}{T} \right) \\ \dot{p}_7 &= -\left(\frac{p_5}{v_{mp}} - \frac{p_7}{T} \right)\end{aligned}\quad (2.38)$$

forms non-homogeneous first order differential equations whose integral result in

$$\begin{aligned}p_6 &= -\frac{p_4}{v_m t_{go}} \left(T t_{go} - T^2 e^{\frac{t_{go}}{T}} + T^2 \right) \\ p_7 &= -\frac{p_5}{v_{mp} t_{go}} \left(T t_{go} - T^2 e^{\frac{t_{go}}{T}} + T^2 \right), \quad v_{mp} \neq 0.\end{aligned}\quad (2.39)$$

Singular interval requires $p_6 = p_7 = 0$, and hence $p_4 = p_5 = 0$ for some finite time interval, which was shown not to exist.

2.4.3 Control-effort-optimal Guidance

The problem is to find a control which transfer a missile from an arbitrary initial position to a target position in minimum consumption of control effort. The optimal criterion is the required control effort which may be formed in either absolute value or squared value in the performance index. The guidance strategy and the method of control law derivation are the same as those of time-optimal guidance. Derivation of an optimal control for this problem is presented below with '*' and arguments except t_f omitted for simplicity where statements are clear.

Control-effort-optimal Guidance for Ideal Model

From (2.12) state equations are given by

$$\begin{aligned}
 \dot{x}_1 &= v_{tp} \cos \psi_t - v_{mp} \cos x_5 \\
 \dot{x}_2 &= v_{tp} \sin \psi_t - v_{mp} \sin x_5 \\
 \dot{x}_3 &= v_t \sin \gamma_t - v_m \sin x_4 \\
 \dot{x}_4 &= \frac{n_\gamma}{v_m} \\
 \dot{x}_5 &= \frac{n_\psi}{v_{mp}}.
 \end{aligned} \tag{2.40}$$

The performance index for this problem is

$$J = \frac{1}{2} (c_1 x_1^2(t_f) + c_2 x_2^2(t_f) + c_3 x_3^2(t_f)) + \int_t^{t_f} \frac{1}{2} (q_1 n_\gamma^2 + q_2 n_\psi^2) dt \tag{2.41}$$

where c_1, c_2, c_3, q_1 and q_2 are some positive values which are to weigh penalties on each associated parameters.

The Hamiltonian is

$$\begin{aligned}
 H(t) &= \frac{q_1}{2} n_\gamma^2 + \frac{q_2}{2} n_\psi^2 + p_1 (v_{tp} \cos \psi_t - v_{mp} \cos x_5) \\
 &+ p_2 (v_{tp} \sin \psi_t - v_{mp} \sin x_5) \\
 &+ p_3 (v_t \sin \gamma_t - v_m \sin x_4) \\
 &+ p_4 \left(\frac{n_\gamma}{v_m} \right) + p_5 \left(\frac{n_\psi}{v_{mp}} \right)
 \end{aligned}$$

To satisfy the necessary condition (2.8), the first derivative of the Hamiltonian with respect to an optimal control must be zero and its second derivative is to be positive definite, which is

$$\begin{aligned} \frac{\partial H}{\partial n_\gamma} = 0 &= q_1 n_\gamma + \frac{p_4}{v_m}, & \left(\frac{\partial^2 H}{\partial n_\gamma^2} = q_1 > 0 \right) \\ \frac{\partial H}{\partial n_\psi} = 0 &= q_2 n_\psi + \frac{p_5}{v_{mp}}, & \left(\frac{\partial^2 H}{\partial n_\psi^2} = q_2 > 0 \right). \end{aligned} \quad (2.42)$$

Then the optimal control is

$$\begin{aligned} n_\gamma &= -\frac{p_4}{q_1 v_m} \\ n_\psi &= -\frac{p_5}{q_2 v_{mp}}. \end{aligned} \quad (2.43)$$

From the costate equations and the boundary conditions it is easily derived that

$$\begin{aligned} p_1 &= c_1 x_1(t_f) \\ p_2 &= c_2 x_2(t_f) \\ p_3 &= c_3 x_3(t_f) \end{aligned} \quad (2.44)$$

and p_4 and p_5 are same as (2.32)(2.33). One problem associated with this formula is that, p_4 and p_5 approach zero as t_{go} does, which results in the decrease of control, and the guidance may not generate enough control efforts about the final interception stage. This can be made up with the adjustments of weighted penalty coefficients such as

$$\begin{aligned} c_1, c_2, c_3 &= \frac{\text{positive constant}}{t_{go}} \\ q_1, q_2 &= \text{positive constant} \cdot t_{go} \end{aligned} \quad (2.45)$$

which is to weigh more penalty on the estimated final states and less on the control as t_{go} approaches zero.

Control-effort-optimal Guidance with Response Delay

Again the response delay caused by the first order missile system dynamics described in (2.35) is considered.

State equations are given by

$$\begin{aligned}
 \dot{x}_1 &= v_{tp} \cos \psi_t - v_{mp} \cos x_5 \\
 \dot{x}_2 &= v_{tp} \sin \psi_t - v_{mp} \sin x_5 \\
 \dot{x}_3 &= v_t \sin \gamma_t - v_m \sin x_4 \\
 \dot{x}_4 &= \frac{\bar{n}_\gamma}{v_m} \\
 \dot{x}_5 &= \frac{\bar{n}_\psi}{v_{mp}} \\
 \dot{\bar{n}}_\gamma &= \frac{n_\gamma - \bar{n}_\gamma}{T} \\
 \dot{\bar{n}}_\psi &= \frac{n_\psi - \bar{n}_\psi}{T}.
 \end{aligned}$$

This case the Hamiltonian is

$$\begin{aligned}
 H(t) &= \frac{q_1}{2} n_\gamma^2 + \frac{q_2}{2} n_\psi^2 + p_1 (v_{tp} \cos \psi_t - v_{mp} \cos x_5) \\
 &+ p_2 (v_{tp} \sin \psi_t - v_{mp} \sin x_5) + p_3 (v_t \sin \gamma_t - v_m \sin x_4) \\
 &+ p_4 \left(\frac{\bar{n}_\gamma}{v_m} \right) + p_5 \left(\frac{\bar{n}_\psi}{v_{mp}} \right) + p_6 \left(\frac{n_\gamma - \bar{n}_\gamma}{T} \right) + p_7 \left(\frac{n_\psi - \bar{n}_\psi}{T} \right) \quad (2.46)
 \end{aligned}$$

and requirements for the necessary condition is

$$\begin{aligned}
 \frac{\partial H}{\partial n_\gamma} = 0 &= q_1 n_\gamma + \frac{p_6}{v_m}, \quad \left(\frac{\partial^2 H}{\partial n_\gamma^2} = q_1 > 0 \right) \\
 \frac{\partial H}{\partial n_\psi} = 0 &= q_2 n_\psi + \frac{p_7}{v_{mp}}, \quad \left(\frac{\partial^2 H}{\partial n_\psi^2} = q_2 > 0 \right). \quad (2.47)
 \end{aligned}$$

Then control law is decided to be

$$\begin{aligned}
 n_\gamma &= -\frac{p_6}{q_1 v_m} \\
 n_\psi &= -\frac{p_7}{q_2 v_{mp}}. \quad (2.48)
 \end{aligned}$$

Costates $p_1 - p_5$ are same as defined for the ideal case and p_6 and p_7 are same as (2.39).

2.4.4 A Note on the Derivation of \dot{p}_4, \dot{p}_5

The missile velocity component projected on ψ plane, $v_{mp} = v_m \cos \gamma_m$, was assumed constant in the derivation of \dot{p}_4, \dot{p}_5 in (2.20)(2.21), which was to separate control action in each γ, ψ direction. In this way n_γ is solely based on kinematics in γ plane, and n_ψ only depends on the components in ψ plane, as can be seen in (2.16)(2.20)(2.21).

A different and mathematically more rigorous approach is to regard v_{mp} as a function of $\gamma_m(x_4)$. For instances for time-optimal case, this approach defines the Hamiltonian to be

$$\begin{aligned} H = & 1 + p_1(v_{tp} \cos \psi_t - v_m \cos x_4 \cos x_5) \\ & + p_2(v_{tp} \sin \psi_t - v_m \cos x_4 \sin x_5) \\ & + p_3(v_t \sin \gamma_t - v_m \sin x_4) \\ & + p_4 \left(\frac{n_{max}}{v_m} u_\gamma \right) + p_5 \left(\frac{n_{max}}{v_m \cos x_4} u_\psi \right). \end{aligned}$$

From the necessary condition

$$\begin{aligned} \dot{p}_4 = -\frac{\partial H}{\partial x_4} &= -(p_1 v_m \sin x_4 \cos x_5 + p_2 v_m \sin x_4 \sin x_5 \\ &\quad - p_3 v_m \cos x_4 + p_5 \frac{n_{max}}{v_m} u_\psi \sec x_4 \tan x_4) \\ \dot{p}_5 = -\frac{\partial H}{\partial x_5} &= -(p_1 v_m \cos x_4 \sin x_5 - p_2 v_m \cos x_4 \cos x_5) \end{aligned} \quad (2.49)$$

which is comparable with (2.20)(2.21). In (2.49) \dot{p}_4 and hence p_4 contains p_5 and u_ψ , so the control sequence will be $p_5 \rightarrow u_\psi \rightarrow p_4 \rightarrow u_\gamma$. It is not presented in this paper, but simulation results showed that both approaches result in identical guidance law not only in miss distance but in the behavior of every system parameter. This can be considered as an example of non-uniqueness of optimal controls [16]. Resultant equations from this variable v_{mp} approach are more complicated. Hence, giving preference to the simpler controller constant, v_{mp} driven equations are selected in this research.

2.4.5 Derivation of \dot{x} from Range and Angle Information

In derivation of the optimal guidance law presented in this paper, missile-target relative distances along the reference axis, (x_1, x_2, x_3) , were selected as states. Costates which are required to determine control were also defined with those states. In practice, information provided by missile inertial navigation system is range and LOS angle related parameters [7]. For this reason, and in the consideration of practical implementation, a way to derive \dot{x}_1, \dot{x}_2 and \dot{x}_3 from range and LOS angle related measurements is studied in this section. Consider Figure (2.3) (b) and (d), where it is defined that

$$\begin{aligned} v_{mh} &= v_{m/\theta} \cos \gamma_{m/\theta} = v_m \cos \gamma_m \cos(\psi_m - \phi) \\ v_{mv} &= v_{m/\theta} \sin \gamma_{m/\theta}. \end{aligned} \quad (2.50)$$

Then, from Figure (2.3)(b) v_{mh} and v_{mv} can be derived from v_{mr} and $v_{m\theta}$

$$\begin{aligned} v_{mh} &= v_{mr} \cos \theta - v_{m\theta} \sin \theta \\ v_{mv} &= v_{mr} \sin \theta - v_{m\theta} \cos \theta \end{aligned} \quad (2.51)$$

and from Figure (2.3)(a)(d)

$$\begin{aligned} v_{m1} &= v_{mh} \cos \phi - v_{m\phi} \sin \phi \\ v_{m2} &= v_{mh} \sin \phi - v_{m\phi} \cos \phi \\ v_{m3} &= v_m \sin \gamma_m. \end{aligned} \quad (2.52)$$

Target velocity components $v_{th} v_{tv} v_{t1} v_{t2} v_{t3}$ is defined in the same way with subscript m replaced by t . With (2.51)(2.52) $\dot{x}_1 - \dot{x}_3$ is defined as shown below.

$$\begin{aligned} \dot{x}_1 &= v_{t1} - v_{m1} \\ &= v_{th} \cos \phi - v_{t\phi} \sin \phi - v_{mh} \cos \phi - v_{m\phi} \sin \phi \\ &= (v_{th} - v_{mh}) \cos \phi - (v_{t\phi} - v_{m\phi}) \sin \phi \end{aligned}$$

$$\begin{aligned}
&= (v_{tr} \cos \theta - v_{t\theta} \sin \theta - v_{mr} \cos \theta - v_{m\theta} \sin \theta) \cos \phi - (v_{t\phi} - v_{m\phi}) \sin \phi \\
&= ((v_{tr} - v_{mr}) \cos \theta - (v_{t\theta} - v_{m\theta}) \sin \theta) \cos \phi - (v_{t\phi} - v_{m\phi}) \sin \phi \\
&= (\dot{r} \cos \theta - r\dot{\theta} \sin \theta) \cos \phi - r\dot{\phi} \cos \theta \sin \phi \tag{2.53}
\end{aligned}$$

$$\begin{aligned}
\dot{x}_2 &= v_{t2} - v_{m2} \\
&= v_{th} \sin \phi - v_{t\phi} \cos \phi - v_{mh} \sin \phi - v_{m\phi} \cos \phi \\
&= (v_{th} - v_{mh}) \sin \phi - (v_{t\phi} - v_{m\phi}) \cos \phi \\
&= (\dot{r} \cos \theta - r\dot{\theta} \sin \theta) \sin \phi - r\dot{\phi} \cos \theta \cos \phi \tag{2.54}
\end{aligned}$$

$$\begin{aligned}
\dot{x}_3 &= v_{t3} - v_{m3} = v_{tv} - v_{mv} \\
&= v_{tr} \sin \theta - v_{t\theta} \cos \theta - v_{mr} \sin \theta - v_{m\theta} \cos \theta \\
&= (v_{tr} - v_{mr}) \sin \theta + (v_{t\theta} - v_{m\theta}) \cos \theta \\
&= \dot{r} \sin \theta - r\dot{\theta} \cos \theta. \tag{2.55}
\end{aligned}$$

This relation was used in the optimal guidance simulation in this research.

2.5 Sliding Mode Guidance Law

2.5.1 Brief Review of Sliding Mode Control Problem

Sliding mode control is a type of *variable structure control*(VSC) which can change the structure of a system intentionally during the transient control process in order to improve overall control characteristics. Another example of this VSC is the *bang-bang control* whose control is defined by a rapid switching between two maximum admissible values. The main and most significant distinction between the two may lie on two facts: sliding mode generates control whose magnitude is variable and provides deterministic control of uncertain systems. Sliding mode control is briefly reviewed in this section. Details can be referred from references such as [8, 13, 24, 26] which provide comprehensive tutorials of the sliding mode control in theory and design

methodology.

Consider a general nonlinear system given by

$$\dot{\mathbf{x}}(t) = \mathbf{f}(\mathbf{x}(t), \mathbf{u}(t), t)$$

where $\mathbf{x}(t) \in R^n$ is the state, $\mathbf{u}(t) \in R^m$ is the control. Sliding mode control is to find a switching surface (*sliding surface*) $\mathbf{S}(\mathbf{x})$ and a discontinuous control law

$$\begin{aligned} \mathbf{u}(\mathbf{x}, t) &= \mathbf{u}^+(\mathbf{x}, t) \text{ if } \mathbf{S}(\mathbf{x}) > 0 \\ &= \mathbf{u}^-(\mathbf{x}, t) \text{ if } \mathbf{S}(\mathbf{x}) < 0 \end{aligned} \quad (2.56)$$

so that state $\mathbf{x}(t)$ outside the sliding surface is driven on to the surface $\mathbf{S}(\mathbf{x}) = 0$. Given the sliding surface is invariant, once states reaches, they remain on the surface thereafter and the system dynamics is solely governed by the sliding surface $\mathbf{S}(\mathbf{x}) = 0$. This motion of states along the surface $\mathbf{S}(\mathbf{x}) = 0$ is called *sliding mode*.

Accordingly design of sliding mode control is mainly divided to two parts. The first is the choice of sliding surface $\mathbf{S}(\mathbf{x}) = C\mathbf{x}$ which should have some desirable characteristics in order to steer states to the desired location. The second is the determination of a discontinuous control which gurarantees the existence of sliding modes and the invariance of the sliding surface, and drive the states from arbitrary initial position to the sliding surface in finite time, In the selection of $\mathbf{S}(\mathbf{x}) = C\mathbf{x}$, the coefficient C cannot be chosen freely in that system response depends on it. Pole placement technique or optimal logic may be used to design C [8]. The existence of sliding modes are closely related with the convergence of the states to the sliding surface $\mathbf{S}(\mathbf{x}) = 0$ (reaching condition) [25], and hence Lyapunov stability theorem can be used to construct the sliding mode control. The reaching condition is satisfied if [13]

$$V(\mathbf{S}(\mathbf{x})) > 0 \text{ and } \frac{dV(\mathbf{S}(\mathbf{x}))}{dt} < 0$$

which also guarantees the invariance of $\mathbf{S}(\mathbf{x}) = 0$. Sliding mode control law is derived from this inequality.

There are two drawbacks in practical implementation of the sliding mode control. One is the chattering phenomenon, high frequency of oscillating motion of states around sliding surface $S(\mathbf{x}) = 0$ caused by nonideal discontinuous control and/or parasitic effects [26]. Several versions of continuous control approximation [25] as well as *boundary layer* approach [22] were suggested. Another drawback is that the upper bound of uncertainties should be known to realize the invariance condition. An adaptation logic can be combined with sliding mode control to estimate the upper bound on line.

2.5.2 Sliding Mode Guidance Law Design

Consider Figure 2.3(a). According to the classical principle of kinematics [10], missile and target acceleration is represented by

$$\begin{aligned} \ddot{r} - r\dot{\theta}^2 - r\dot{\phi}^2 \cos^2 \theta &= a_{tr} - a_{mr} \\ r\ddot{\theta} + 2\dot{r}\dot{\theta} + r\dot{\phi}^2 \cos \theta \sin \theta &= a_{t\theta} - a_{m\theta} \\ r\ddot{\phi} \cos \theta + 2\dot{r}\dot{\phi} \cos \theta - 2r\dot{\theta}\dot{\phi} \sin \theta &= a_{t\phi} - a_{m\phi}. \end{aligned} \quad (2.57)$$

From Figure 2.3(b) and (d), it is derived that

$$\begin{aligned} a_{m\theta} &= n_\theta \cos(\gamma_{m/\theta} - \theta) \\ a_{m\phi} &= n_\phi \cos(\psi_m - \phi) \end{aligned} \quad (2.58)$$

where $\gamma_{m/\theta}$ is derived in 2.2.

The choice of the sliding surface gives radical affects to the system response. Probably the most common choice of the surface is [22]

$$s(x, t) = \left(\frac{d}{dt} + c \right)^{n-1} x$$

where n is the order of the system and c is strictly positive definite. This sliding surface has proved its effectiveness in various fields, both in regulator problems where control

is to drive the states to the origin and in tracking problems in which the control steers the states to follow desired states. Guidance problem with LOS angles as its states is not necessarily to be a regulator problem or a tracking problem. Holding constant LOS angle strategy achieves zero-miss guidance with even optimal characteristic as described about Figure 2.4. Though the optimality was stated for a non-maneuvering target with constant velocity, it holds for a maneuvering target, too (this optimality will be discussed more in analysis section). This research selects the sliding surface to be

$$s_1 = \dot{\theta}, \quad s_2 = \dot{\phi} \quad (2.59)$$

which is based on basic guidance strategy of PNG and is to keep constant LOS angles, θ and ϕ . From (2.57), $\ddot{\theta}$ and $\ddot{\phi}$ are reorganized to

$$\begin{aligned} \ddot{\theta} &= \frac{-2\dot{r}\dot{\theta} - r\dot{\phi}^2 \cos \theta \sin \theta + a_{t\theta} - a_{m\theta}}{r} \\ \ddot{\phi} &= \frac{-2\dot{r}\dot{\phi} \cos \theta + 2r\dot{\theta}\dot{\phi} \sin \theta + a_{t\phi} - a_{m\phi}}{r \cos \theta}. \end{aligned} \quad (2.60)$$

where $a_{t\theta}$ and $a_{t\phi}$ are target acceleration components which are unknown values and hence can be regarded as disturbances or unmodeled dynamics. Additionally there possibly exist parameter uncertainties and disturbances in the system (2.57). Given *matching condition* is satisfied, all the uncertainties and disturbances including target acceleration can be lumped into one uncertain parameter ([8]), and then (2.60) can be rewritten as

$$\begin{aligned} \ddot{\theta} &= \frac{-2\dot{r}\dot{\theta} - r\dot{\phi}^2 \cos \theta \sin \theta + D_1 - a_{m\theta}}{r} \\ \ddot{\phi} &= \frac{-2\dot{r}\dot{\phi} \cos \theta + 2r\dot{\theta}\dot{\phi} \sin \theta + D_2 - a_{m\phi}}{r \cos \theta} \end{aligned} \quad (2.61)$$

where D_1 and D_2 are the lumped uncertainties. Assume D_1 and D_2 are bounded by constants c_{10} and c_{20} respectively so that

$$\|D_1\| \leq c_{10}, \quad \|D_2\| \leq c_{20}. \quad (2.62)$$

From (2.58)(2.59)(2.61) it can be derived that

$$\begin{aligned} \dot{s}_1 &= \ddot{\theta} = \frac{-2\dot{r}\dot{\theta} - r\dot{\phi}^2 \cos \theta \sin \theta + D_1 - n_\theta \cos(\gamma_{m/\theta} - \theta)}{r} \\ \dot{s}_2 &= \ddot{\phi} = \frac{-2\dot{r}\dot{\phi} \cos \theta + 2r\dot{\theta}\dot{\phi} \sin \theta + D_2 - n_\phi \cos(\psi_m - \phi)}{r \cos \theta}. \end{aligned} \quad (2.63)$$

Take the missile acceleration command to be

$$\begin{aligned} n_\theta &= \frac{-2\dot{r}\dot{\theta} - r\dot{\phi}^2 \cos \theta \sin \theta + k_1 \text{sgn}(s_1)}{n_\theta \cos(\gamma_{m/\theta} - \theta)} \\ n_\phi &= \frac{-2\dot{r}\dot{\phi} \cos \theta + 2r\dot{\theta}\dot{\phi} \sin \theta + k_2 \text{sgn}(s_2)}{n_\phi \cos(\psi_m - \phi)}. \end{aligned} \quad (2.64)$$

Inserting (2.64) into (2.63) yields

$$\begin{aligned} \dot{s}_1 &= \frac{D_1 - k_1 \text{sgn}(s_1)}{r} \\ \dot{s}_2 &= \frac{D_2 - k_2 \text{sgn}(s_2)}{r \cos \theta}. \end{aligned} \quad (2.65)$$

If $k_1 > D_1$ and $k_2 > D_2$, then $s_1 \dot{s}_1 < 0$ and $s_2 \dot{s}_2 < 0$ are achieved and the reaching condition is satisfied. But the D_1 and D_2 are unknown. An adaptation technique can be used to identify the upper bound of the unknown parameters, c_{10} and c_{20} , on-line in recursive manner and set control gains accordingly so that $k_1 > D_1$ and $k_2 > D_2$ are maintained. One problem associated with such an adaptation method is the accumulation of estimated data and the continuous increase of control gains as the result. Too much high control gain can cause chattering, or requires thicker boundary layer which means loose error tolerance for the performance to be adopted. To prevent control from having too much high gain, data forgetting concept [22] may be used to forget past estimated data in a time span and newly estimate parameters after that recursively. In this paper an adaptation logic for the sliding mode gain is proposed which adjusts the magnitude of the gain according to the system response so that too much high control gains are prevented.

Choose k_1 and k_2 to be

$$k_1 = \bar{c}_{10} + c_{11}|s_1|, \quad k_2 = \bar{c}_{20} + c_{21}|s_2| \quad (2.66)$$

where $\bar{c}_{10}, \bar{c}_{20}, c_{11}, c_{21}$ are adaptive parameters which are to be strictly positive definite and assumed to be continuous. Now consider an adaptation logic

$$\begin{aligned}\dot{\tilde{c}}_{10} &= q_{10}r|s_1|, & \dot{c}_{11} &= q_{11}r|s_1| \\ \dot{\tilde{c}}_{20} &= q_{20}\frac{r}{\cos\theta}|s_2|, & \dot{c}_{21} &= q_{21}\frac{r}{\cos\theta}|s_2|.\end{aligned}\quad (2.67)$$

where $\tilde{c}_{10} = \bar{c}_{10} - c_{10}$ and $\tilde{c}_{20} = \bar{c}_{20} - c_{20}$ are estimation error of the lumped uncertainties, and q_{10}, q_{11}, q_{20} , and q_{21} are positive constants which determine the adaptation rate. As c_{10} and c_{20} are constant, $\dot{\tilde{c}}_{10} = \dot{\bar{c}}_{10}$ and $\dot{\tilde{c}}_{20} = \dot{\bar{c}}_{20}$, and so from (2.67) the adaptation law is given by

$$\begin{aligned}\dot{\bar{c}}_{10} &= q_{10}r|s_1|, & \dot{c}_{11} &= q_{11}r|s_1| \\ \dot{\bar{c}}_{20} &= q_{20}\frac{r}{\cos\theta}|s_2|, & \dot{c}_{21} &= q_{21}\frac{r}{\cos\theta}|s_2|.\end{aligned}\quad (2.68)$$

Adaptive parameters are obtained by integrating (2.68)

$$\begin{aligned}\bar{c}_{10} &= \bar{c}_{10}(0) + q_{10} \int r|s_1|, & c_{11} &= c_{11}(0) + q_{11} \int r|s_1| \\ \bar{c}_{20} &= \bar{c}_{20}(0) + q_{20} \int \frac{r}{\cos\theta}|s_2|, & c_{21} &= c_{21}(0) + q_{21} \int \frac{r}{\cos\theta}|s_2|.\end{aligned}\quad (2.69)$$

It is proposed that, given $r > 0$, $\dot{r} < 0$, $\cos\theta > 0$, the sliding surface $s_1 = 0$ and $s_2 = 0$ are asymptotically stable by the control law (2.64) with the control gain defined in (2.66) and the adaptation law (2.68). The proof is given below.

proof Consider the Lyapunov function candidate

$$V = \frac{1}{2}(r^2(s_1^2 + s_2^2) + q_{10}^{-1}\tilde{c}_{10}^2 + q_{20}^{-1}\tilde{c}_{20}^2).\quad (2.70)$$

With (2.65)(2.66) the time derivative of the Lyapunov function yields

$$\begin{aligned}\dot{V} &= r\dot{r}(s_1^2 + s_2^2) + r^2(s_1\dot{s}_1 + s_2\dot{s}_2) + q_{10}^{-1}\tilde{c}_{10}\dot{\tilde{c}}_{10} + q_{20}^{-1}\tilde{c}_{20}\dot{\tilde{c}}_{20} \\ &= r\dot{r}(s_1^2 + s_2^2) + r^2\left(s_1\frac{D_1 - k_1\text{sgn}(s_1)}{r} + s_2\frac{D_2 - k_2\text{sgn}(s_2)}{r\cos\theta}\right) \\ &\quad + q_{10}^{-1}\tilde{c}_{10}\dot{\tilde{c}}_{10} + q_{20}^{-1}\tilde{c}_{20}\dot{\tilde{c}}_{20} \\ &= r\dot{r}(s_1^2 + s_2^2) + r(s_1D_1 - k_1|s_1| + \frac{s_2D_2 - k_2|s_2|}{\cos\theta}) + q_{10}^{-1}\tilde{c}_{10}\dot{\tilde{c}}_{10} + q_{20}^{-1}\tilde{c}_{20}\dot{\tilde{c}}_{20}\end{aligned}$$

$$\begin{aligned}
&\leq r\dot{r}(s_1^2 + s_2^2) + r(|s_1||D_1| - k_1|s_1|) + \frac{r}{\cos\theta}(|s_2||D_2| - k_2|s_2|) \\
&\quad + q_{10}^{-1}\tilde{c}_{10}\dot{\tilde{c}}_{10} + q_{20}^{-1}\tilde{c}_{20}\dot{\tilde{c}}_{20} \\
&= r\dot{r}(s_1^2 + s_2^2) + r|s_1||D_1| + \frac{r}{\cos\theta}|s_2||D_2| - rk_1|s_1| - \frac{r}{\cos\theta}k_2|s_2| \\
&\quad + q_{10}^{-1}\tilde{c}_{10}\dot{\tilde{c}}_{10} + q_{20}^{-1}\tilde{c}_{20}\dot{\tilde{c}}_{20} \\
&\leq r\dot{r}(s_1^2 + s_2^2) + r|s_1|c_{10} + \frac{r}{\cos\theta}|s_2|c_{20} - r|s_1|(\bar{c}_{10} + c_{11}|s_1|) \\
&\quad - \frac{r}{\cos\theta}|s_2|(\bar{c}_{20} + c_{21}|s_2|) + q_{10}^{-1}\tilde{c}_{10}\dot{\tilde{c}}_{10} + q_{20}^{-1}\tilde{c}_{20}\dot{\tilde{c}}_{20} \\
&= r\dot{r}(s_1^2 + s_2^2) + r|s_1|(c_{10} - \bar{c}_{10}) + \frac{r}{\cos\theta}|s_2|(c_{20} - \bar{c}_{20}) - r|s_1|^2c_{11} - \frac{r}{\cos\theta}|s_2|^2c_{21} \\
&\quad + q_{10}^{-1}\tilde{c}_{10}\dot{\tilde{c}}_{10} + q_{20}^{-1}\tilde{c}_{20}\dot{\tilde{c}}_{20} \\
&= r\dot{r}(s_1^2 + s_2^2) - r|s_1|\bar{c}_{10} - \frac{r}{\cos\theta}|s_2|\bar{c}_{20} + q_{10}^{-1}\tilde{c}_{10}\dot{\tilde{c}}_{10} + q_{20}^{-1}\tilde{c}_{20}\dot{\tilde{c}}_{20} \\
&\quad - r|s_1|^2c_{11} - \frac{r}{\cos\theta}|s_2|^2c_{21} + (|s_1| - |s_1|)q_{11}^{-1}c_{11}\dot{c}_{11} + (|s_2| - |s_2|)q_{21}^{-1}c_{21}\dot{c}_{21} \\
&= r\dot{r}(s_1^2 + s_2^2) - \bar{c}_{10}(r|s_1| - q_{10}^{-1}\dot{\tilde{c}}_{10}) - \bar{c}_{20}(\frac{r}{\cos\theta}|s_2| - q_{20}^{-1}\dot{\tilde{c}}_{20}) \\
&\quad - c_{11}(r|s_1| - q_{11}^{-1}\dot{c}_{11}) - c_{21}(\frac{r}{\cos\theta}|s_2| - q_{21}^{-1}\dot{c}_{21}) - |s_1|q_{11}^{-1}c_{11}\dot{c}_{11} - |s_2|q_{21}^{-1}c_{21}\dot{c}_{21}.
\end{aligned}$$

With the adaptation logic (2.67) it is concluded that

$$\dot{V} \leq r\dot{r}(s_1^2 + s_2^2) - |s_1|q_{11}^{-1}c_{11}\dot{c}_{11} - |s_2|q_{21}^{-1}c_{21}\dot{c}_{21} < 0$$

for nonzero s_1 and/or s_2 . Thus asymptotic stability of the switching surface $s_1 = 0$ and $s_2 = 0$ was proved. \triangle

The assumption $\dot{r} < 0$ is always valid for any head-on case and for the tail-chasing case where a missile has velocity advantage over a target. $\cos\theta > 0$ is not a rigorous assumption given LOS is initially set in the positive half of the reference axis. The adaptation logic formalized in (2.68) is not intended to estimate the exact upper bound of D_1 and D_2 , rather it maintains $k_1 \geq D_1$ and $k_2 \geq D_2$. In the determination of the adaptation rate, small numbers may be the choice for q_{10} and q_{20} while some large numbers for q_{11} and q_{21} . This choice is to increase control gain rapidly when s is off the sliding surface $s = 0$ so that the increased control can drive s back onto the surface $s = 0$ quickly while maintaining small control gain when s

is on the zero. Different adaptation laws may be derived upon the different choice of Lyapunov function and sliding mode gain k . As examples, adaptive logics for another sliding mode guidance is found in [2], for a robot manipulator in [9], for a general nonlinear system in [27]. When the boundary layer is used for continuous control approximation, then $sgn(\cdot)$ in control law (2.64) is modified to $sat(\cdot)$ which is defined as

$$sat(s) = \begin{cases} sgn(s) & \text{if } |s| \geq \epsilon \\ s/\epsilon & \text{if } |s| < \epsilon, \quad \epsilon > 0 \text{ constant} \end{cases} \quad (2.71)$$

with boundary thickness 2ϵ , where as ϵ approaches zero $sat(s)$ approaches $sgn(s)$.

Chapter 3

Simulation and Analysis

3.1 Simulation and Analysis

Simulation was performed to investigate the effectiveness of the guidance laws: PNG, Time-Optimal Guidance (TOG), Control-effort-Optimal Guidance (COG) and Sliding Mode Guidance (SMG). 2D simulation results are presented followed by 3D simulation results. Nulling one angle definition - either θ or ϕ - from the engagement geometry depicted in Figure 2.3(a) leads to planar engagement model for 2D simulation. The main purpose of the 2D simulation is to investigate the characteristic of each guidance law while the 3D simulation is to compare miss distance.

When it comes to the ideal model, PNG is a perfect guidance law in that it always achieves zero miss distance. Practical limitations and imperfections such as actuator saturation, response delay, noise and other parasitic effects degrade PNG performance and cause a considerable miss distance in some cases. For this reason, comparison of proposed guidance laws in ideal model doesn't make much sense. Among possible limitations, actuator saturation, response delay and noise effect are considered.

To perform simulations, numerical values for missile-target kinematics and specific coefficients of controllers are chosen as follows.

· For kinematics: Missile velocity v_m is $900m/sec$ and target velocity v_t is $300m/sec$

unless noted. It is assumed that maximum target acceleration is $10g$. Current tactical missile is known to have several times higher acceleration capability over target [28], but too high acceleration can increase drag and may reduce the range capability. In this consideration missile maximum acceleration is assumed to be limited by $15g$, 50% higher than that of target. Initial missile-target relative distance is set within the typical seeker acquisition range which is up to $24km$ [15].

- For PNG: Effective navigation ratio of 4 is chosen for PNG.
- For COG: Penalty coefficients for COG are,

$$c_1 = \frac{1}{t_{go}}, c_2 = \frac{1000}{t_{go}}, c_3 = \frac{1000}{t_{go}}$$

$$q_1 = q_2 = 1 \cdot t_{go}.$$

The behind idea of this different choice of c_2 , c_3 from c_1 is to emphasize lateral motion instead of LOS-directional motion.

- For SMG: The boundary layer thickness of 0.001 is used for the continuous control approximation. It is generally known that initial value of adaptive parameters affects the adaptation performance. Without loss of generality, the target is assumed to have at least $2g$ maneuverability and accordingly, with the reason stated in Sec. 2.4.7, coefficients of the adaptation law are chosen to be

$$\bar{c}_{10}(0) = \bar{c}_{20}(0) = 2g$$

$$c_{11}(0) = c_{21}(0) = 0$$

$$q_{10} = q_{20} = 0.1, \quad q_{11} = q_{21} = 2000.$$

- Missile response delay: Unless noted time constant of missile dynamics is assumed 0.2 sec. that causes approximately 1 second of achieved missile response delay.

Missile and target acceleration presented in all figures are their acceleration components perpendicular to LOS. Some graphical presentations of simulation results bear vertical lines at the last instant. The lines are caused when missile is located

right beneath or above target at the final instant and are not related with the performance of guidance laws. Presented miss distances were recorded when missile-target relative distance is of minimum or changes its sign from plus to minus whichever comes first. The sign change in relative distance means missile and target are crossed each other. Missile initial heading error is defined a initial angle deviation of missile velocity vector from the collision triangle in Figure 2.4.

3.2 2D Simulation and Analysis

Some notable characteristics of the optimal and sliding mode guidance laws are examined with simple $10g$ target maneuver, followed by their comparison with PNG for some selected target maneuvers. Noise effect is not considered in this 2D simulation analysis, as the noise is undeterministic and makes it difficult to analyze the characteristics of guidance laws.

3.2.1 Notable Characteristics of Optimal and Sliding Mode Guidance

A. Time-optimal Guidance

TOG results are depicted in Figure 3.1– 3.5.

In Figure 3.1, only acceleration saturation is considered. Estimated final states converge to zero about 3.5 seconds and almost zero miss distance is achieved. But high switching of acceleration between the maximum values is shown. Estimated final states also show chattering around zero.

Acceleration switching can be reduced if a 1st order filter is introduced in the final states estimation. The filter (time constant 0.2 sec.) effect is shown in Figure 3.2, where both acceleration switching and final states chattering are attenuated, but some fluctuation of missile flight pass angle is caused. The filter induced miss distance

increase is negligible in the result, but bigger time constant of the filter causes bigger miss distance though attenuates acceleration switching more.

Missile response delay also provides the filter effect and thus can reduce the acceleration switching as shown in Figure 3.3, where final states estimation and flight path angle get much smoother as well as missile acceleration, and smooth final states converge is found. Bigger system time constant brings more attenuated acceleration switching without severe performance degradation as compared in Figure 3.4 and Figure 3.5, because response delay was considered in the optimization.

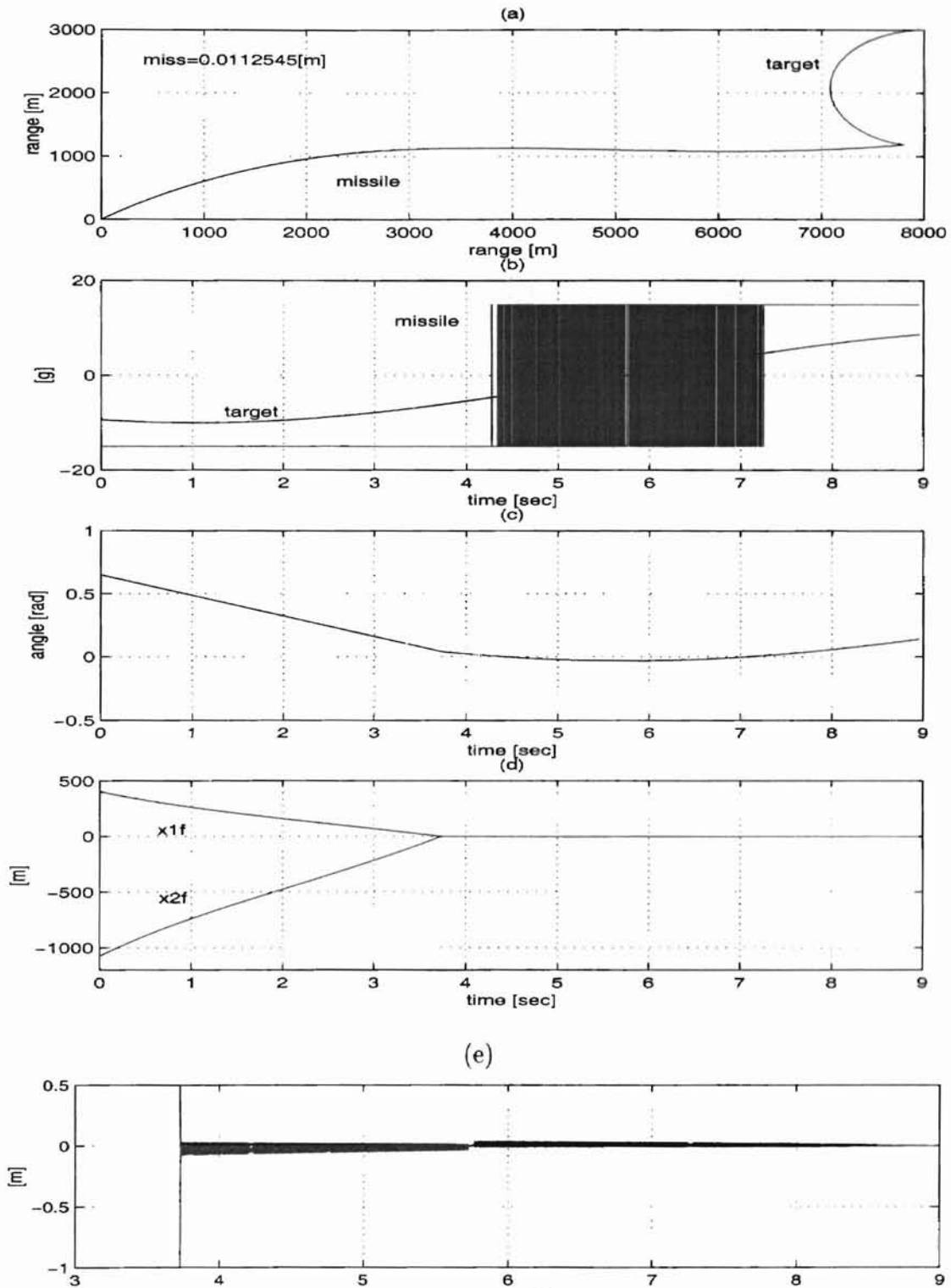


Figure 3.1: TOG for ideal case: (a) Missile-target engagement (b) Acceleration (c) Missile flight path angle (d) Estimated final states (e) Enlargement of (d)

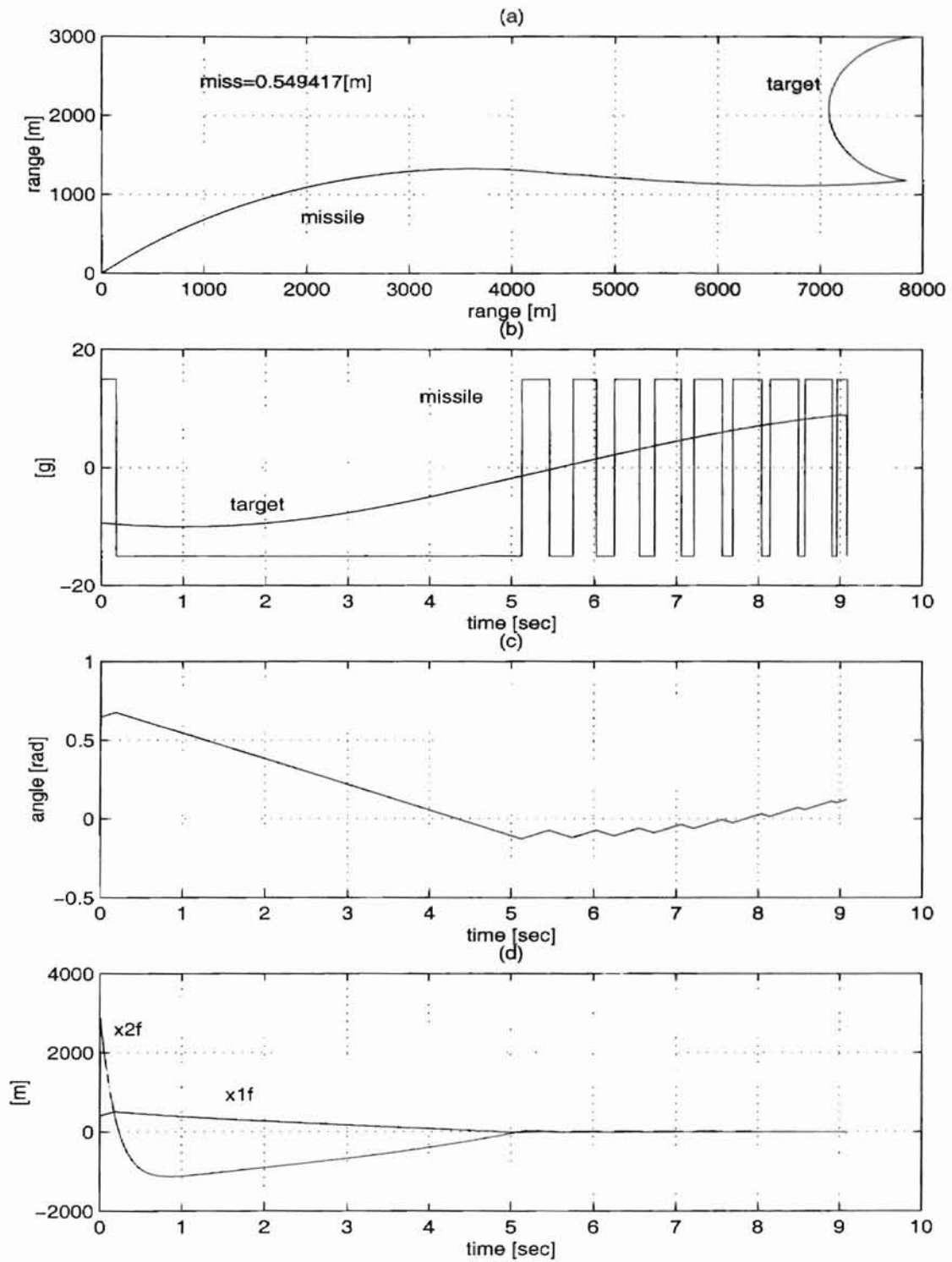


Figure 3.2: TOG with final states estimation filter (filter time constant 0.2 sec.) : (a) Missile-target engagement (b) Acceleration (c) Missile flight path angle (d) Estimated final states

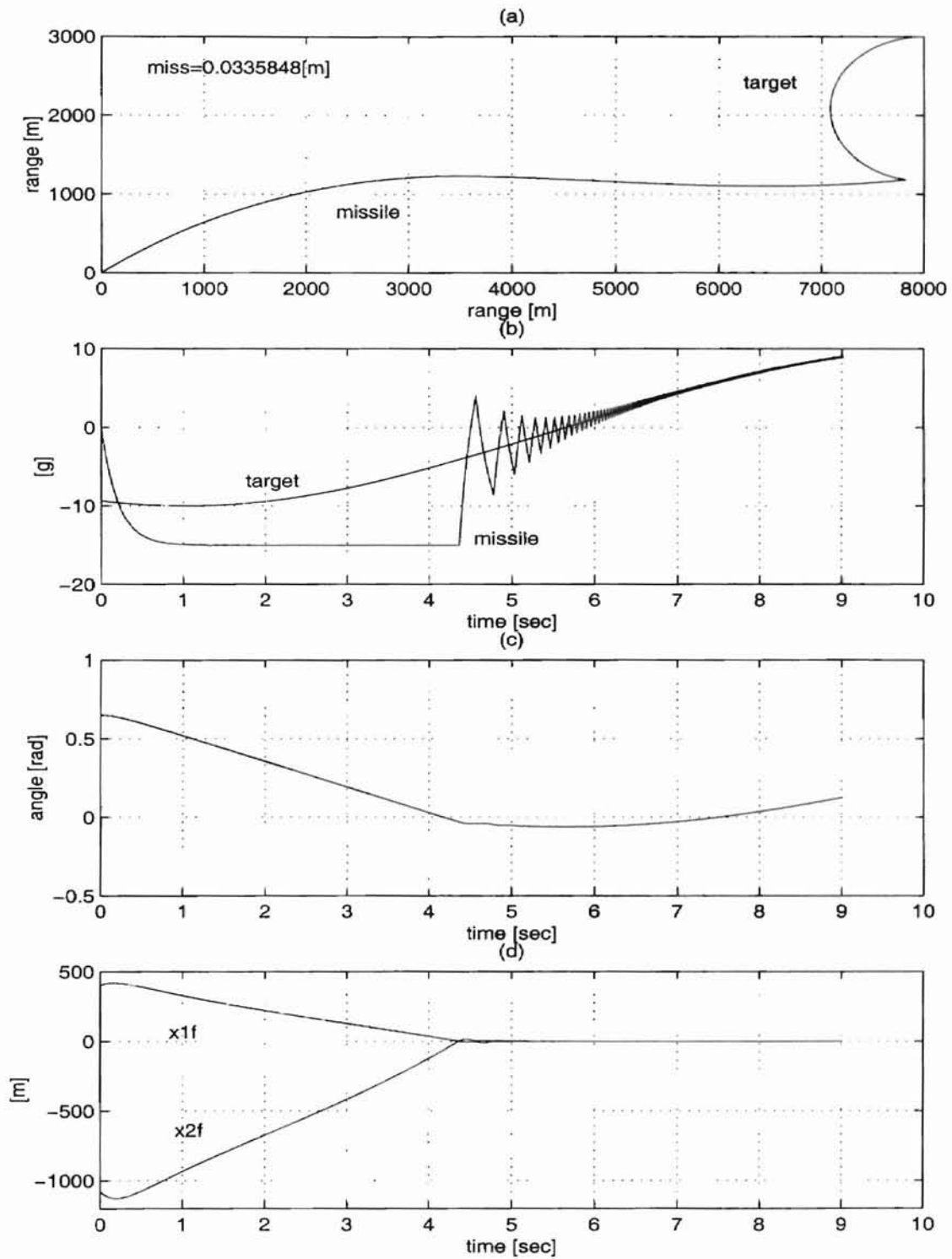


Figure 3.3: TOG with response delay (time constant 0.2 sec.) : (a) Missile-target engagement (b) Acceleration (c) Missile flight path angle (d) Estimated final states

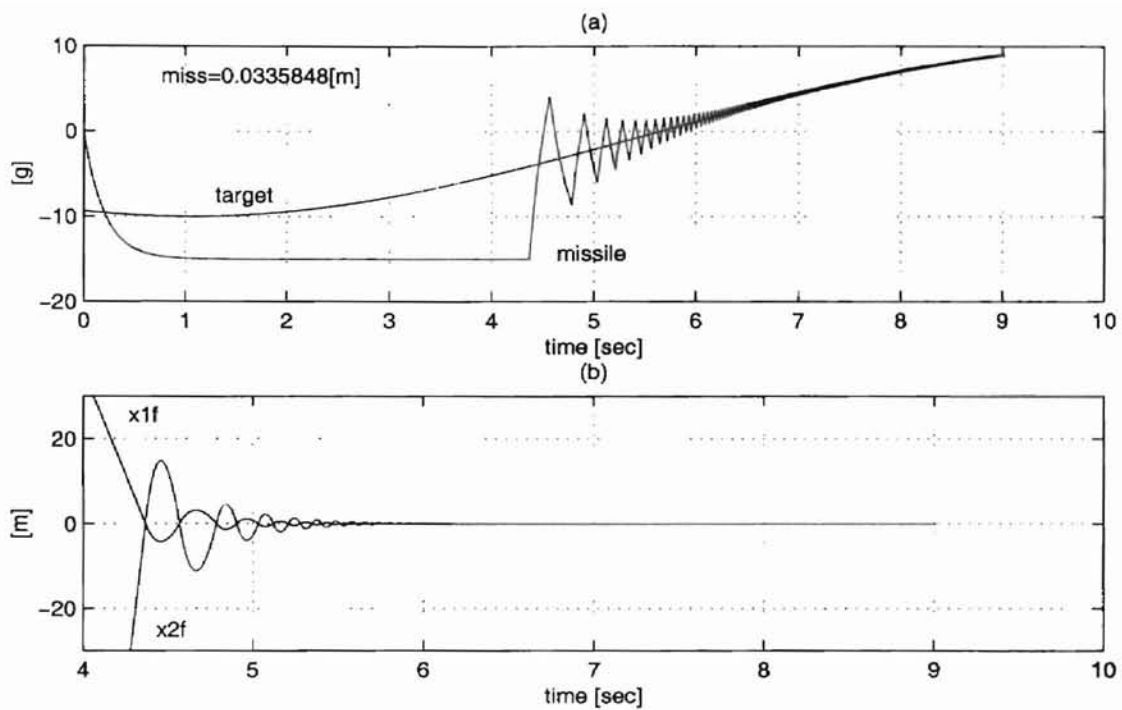


Figure 3.4: TOG with missile dynamics time constant 0.2 sec.: (a) Acceleration (b) Estimated final states

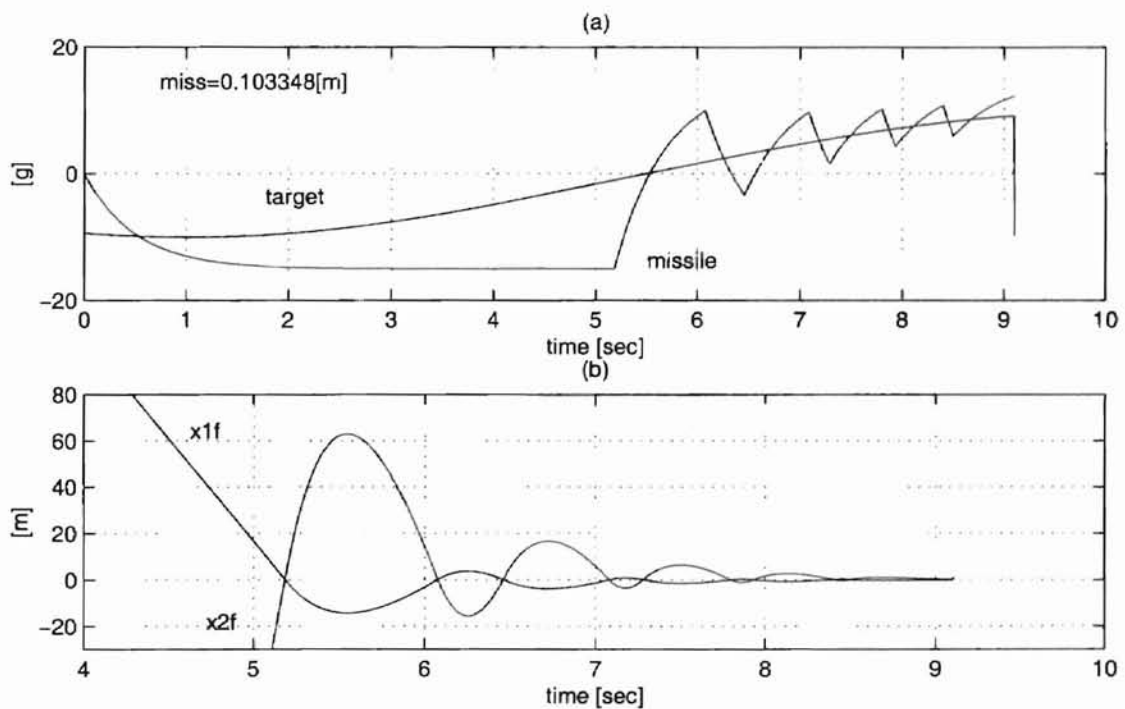


Figure 3.5: TOG with missile dynamics time constant 0.5 sec. : (a) Acceleration (b) Estimated final states

[m]

	10g maneuver			weaving		
	t_{go} error	x_f error	none	t_{go} error	x_f error	none
TOG	10.97	107.55	0.03	5.22	53.94	0.10
COG	15.39	0.04	0.04	36.82	0.01	0.05

Table 3.1: Miss distance caused by t_{go} and x_f estimation error

B. Control-effort-optimal Guidance

COG simulation results are presented in Figure 3.6–3.10. In Figure 3.6 only saturation is considered. The guidance commands maximum control until final states estimation converges to zero, and then follows target acceleration. Switching of acceleration and estimated final states are not shown unlike the TOG case in Figure 3.1.

But response delay causes acceleration chattering which is shown in Figure 3.7 and Figure 3.8. As is the case in TOG, acceleration switching can be attenuated more by introducing bigger system time constant without severe loss of performance.

Figure 3.9 and Figure 3.10 show the difference of missile response upon the choice of penalty coefficients. Constant penalty coefficients (unit for LOS-direction and 1000 for lateral motion) are used in Figure 3.9, and time varying coefficients defined in (2.45) were used in Figure 3.10. Missile acceleration rapidly degrades and final states diverge about the final stage with the constant coefficients, while, with the time varying coefficients, missile acceleration follows target acceleration throughout the interception and final states converge to zero, which results in less miss distance.

Table 3.1 shows the effect of t_{go} estimation error and final state estimation error. -0.1 second of t_{go} error and -100 m of final states estimation error were intentionally included throughout the interception process. COG performance is affected more by t_{go} estimation error while final state estimation error severely degrades TOG

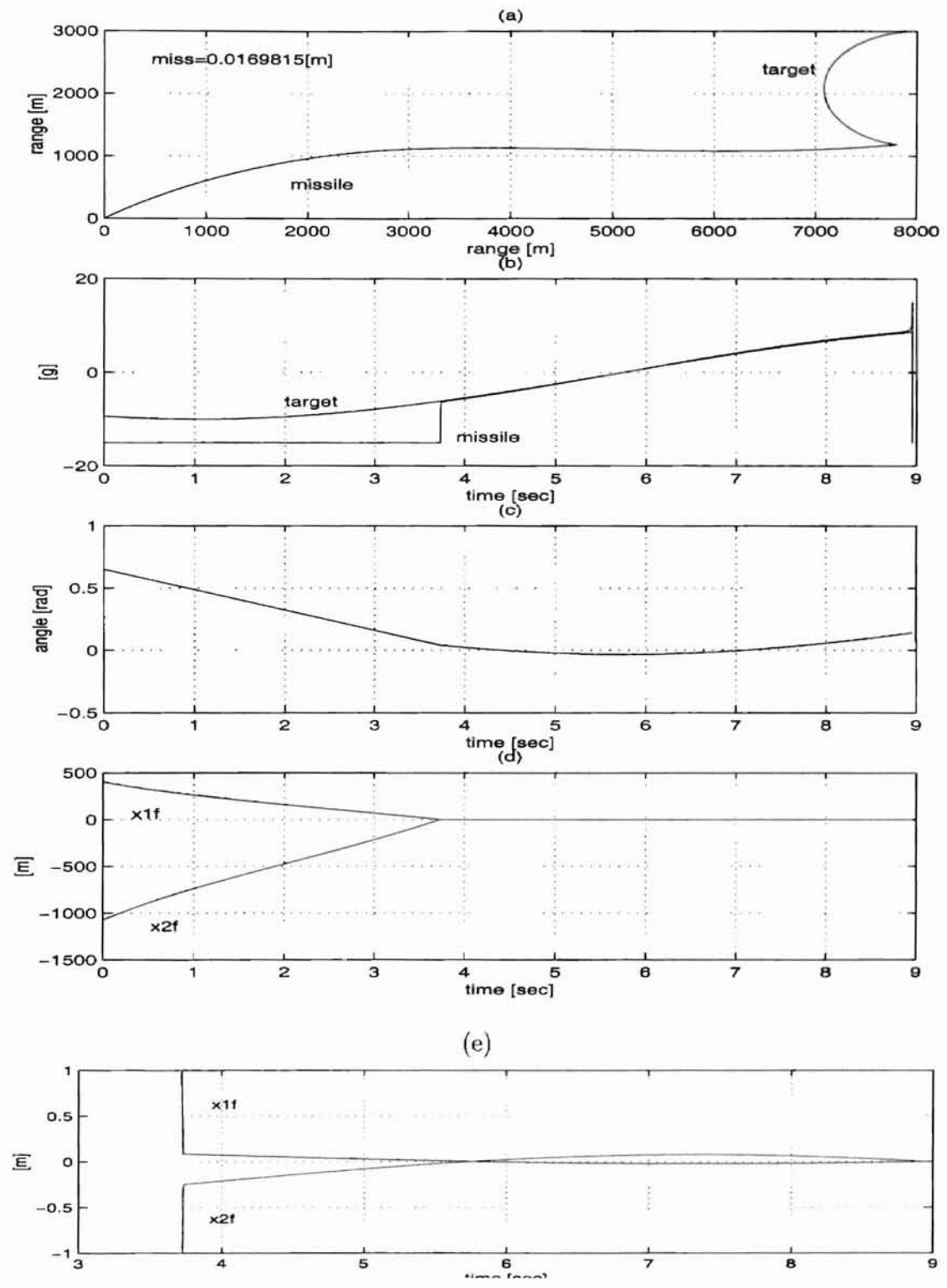


Figure 3.6: COG for simple maneuvering target : (a) Missile-target engagement (b) Acceleration (c) Missile flight path angle (d) Estimated final states (e) Enlargement of (d)

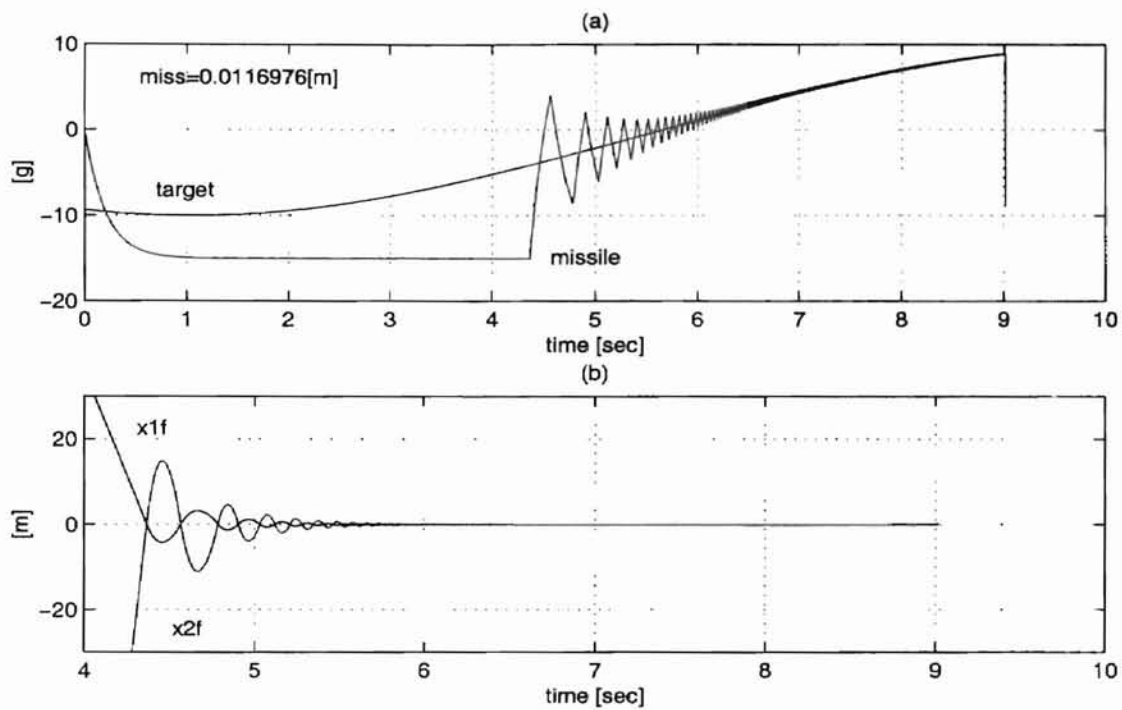


Figure 3.7: COG with missile dynamics time constant 0.2 sec.: (a) Acceleration (b) Estimated final states

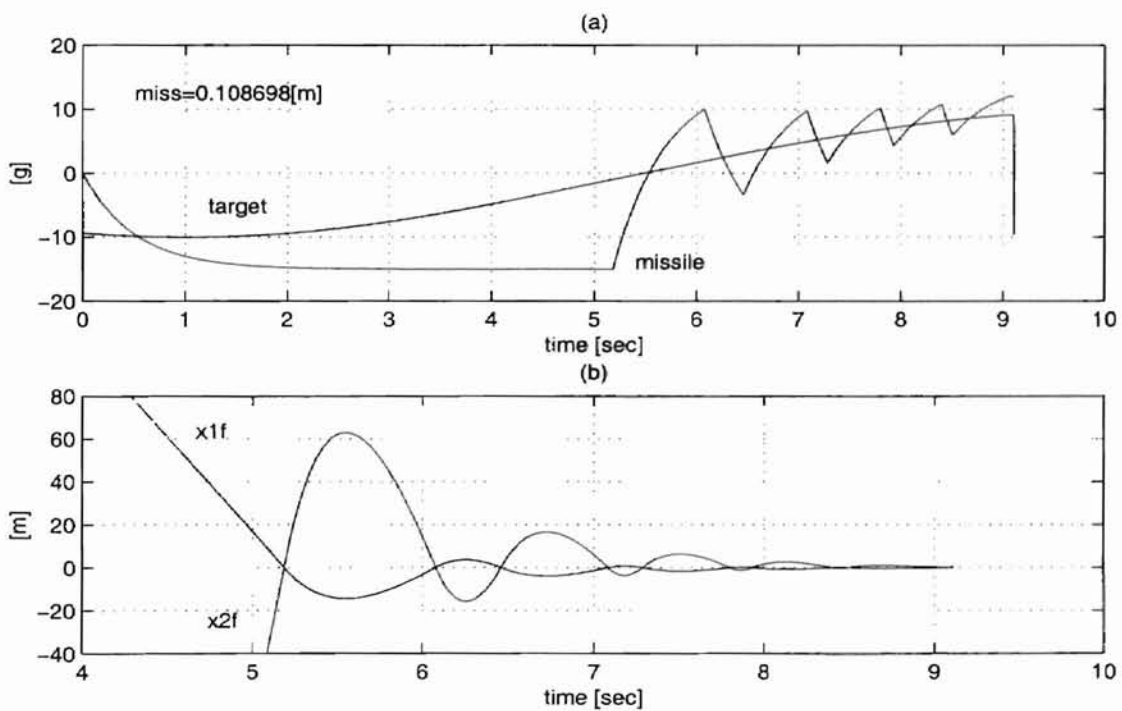


Figure 3.8: COG with missile dynamics time constant 0.5 sec.: (a) Acceleration (b) Estimated final states

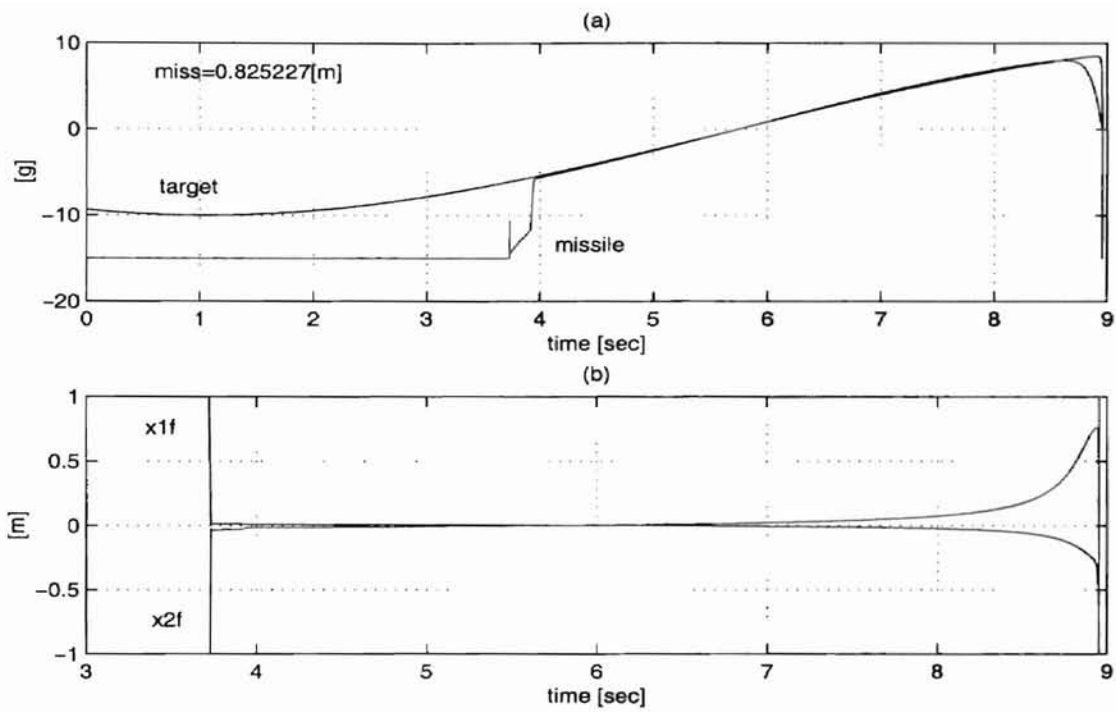


Figure 3.9: COG with constant penalty coefficients : (a) Acceleration (b) Estimated final states

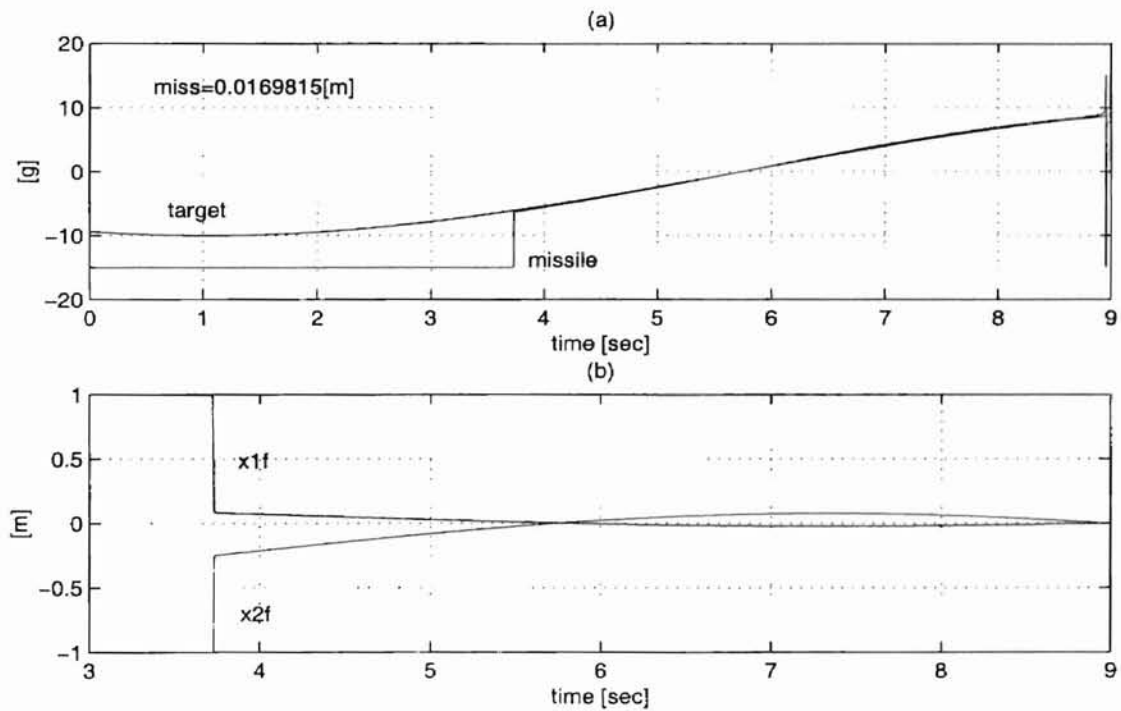


Figure 3.10: COG with time varying penalty coefficients : (a) Acceleration (b) Estimated final states

performance.

C. Sliding Mode Guidance

SMG simulation results for a simple $10g$ target are presented in Figure 3.11– 3.13 where the effectiveness of proposed adaptation law is also found.

It is found in Figure 3.11 that the behavior of control gain k , missile acceleration, and s function are closely related. Control gain increases rapidly at the first stage to drive s towards zero with maximum control effort. After s reaches zero the gain k decrease dramatically to be a bit over the norm of disturbance (i.e. target acceleration). During which the boundary layer contains s in it, the decreased gain k is maintained and the missile acceleration follows target acceleration.

Figure 3.12 gives detail description of control gain $k = c_0 + c_1|s|$ with its adaptive parameters. As is designed, c_1 grows rapidly while c_0 increases slowly. For ideal situation, s will remain zero once it reaches zero during which the adaptive parameters c_0 and c_1 will stop increasing, and then k will be represented by c_0 alone. For the continuous control approximation with the boundary layer, s is not of exact zero because of target maneuvering but stays inside boundary layer, which causes the adaptive parameters keep increasing. But, within the boundary layer, $s \approx 0$ attenuates the parameter increasing rate to be negligibly small and leads rapid decrease of $c_1|s|$, and hence the decrease of k .

Figure 3.13 shows the behavior of control gain k and the missile acceleration when the missile has no initial heading error, which is comparable with Figure 3.11 (b)(c). s is off zero because of target maneuvering but soon driven back into boundary layer by increased gain k . The adaptation rate is a bit slower than the case with initial heading error.

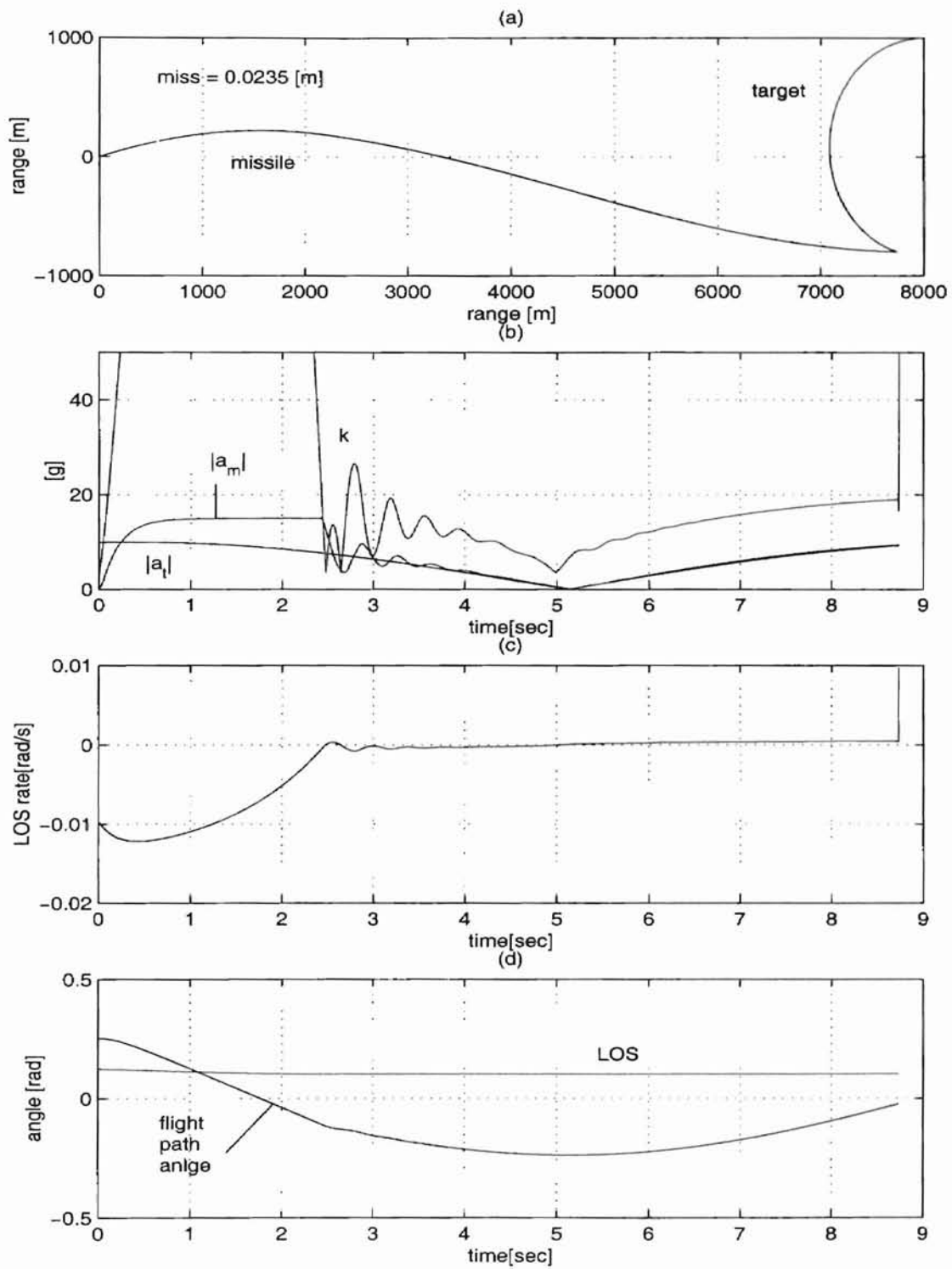


Figure 3.11: SMG for a simple target: (a) Missile-target engagement (b) Acceleration and control gain k (c) s function (LOS rate) (d) Missile flight path angle and LOS angle

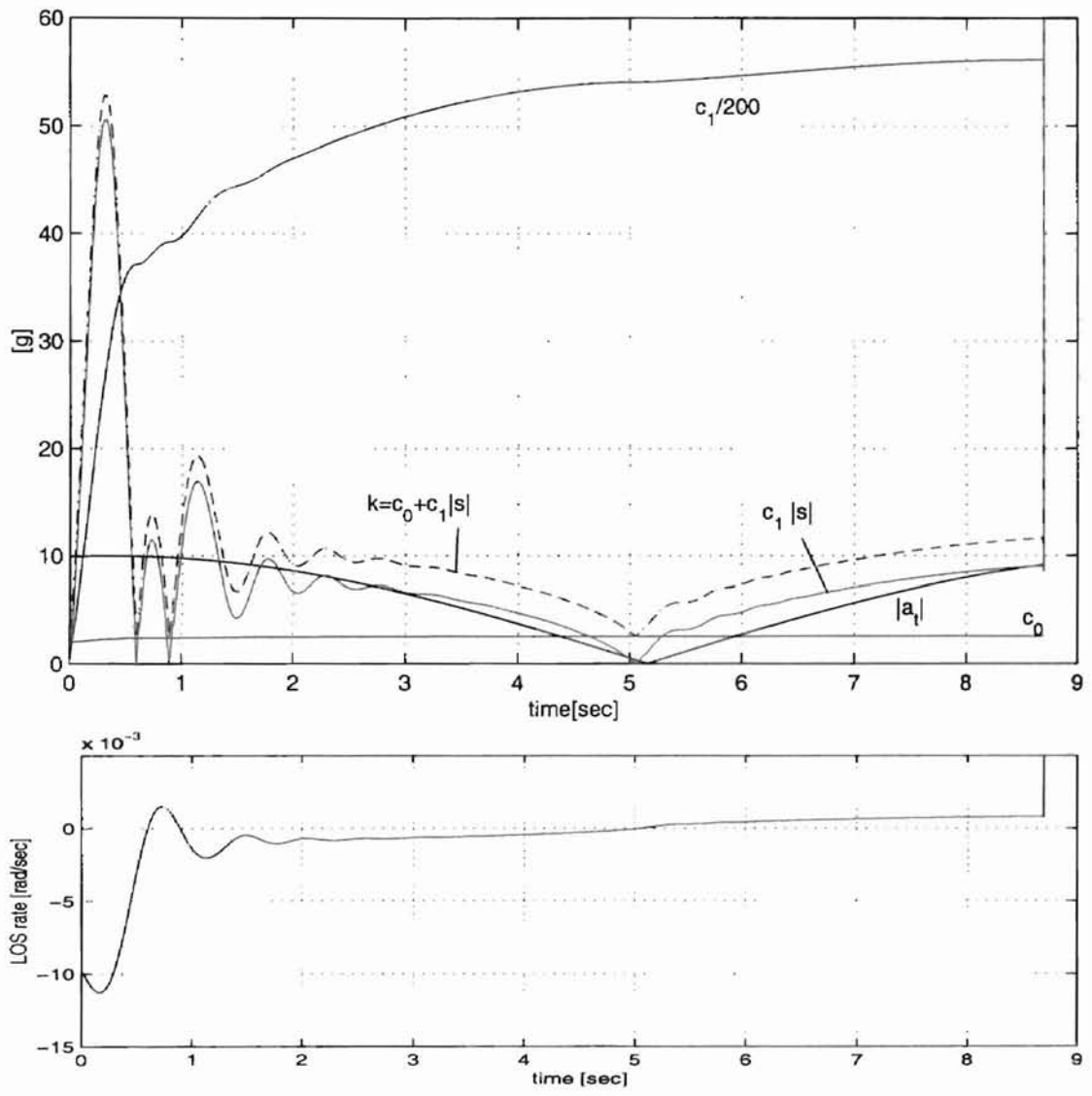


Figure 3.12: Adaptation parameters and s

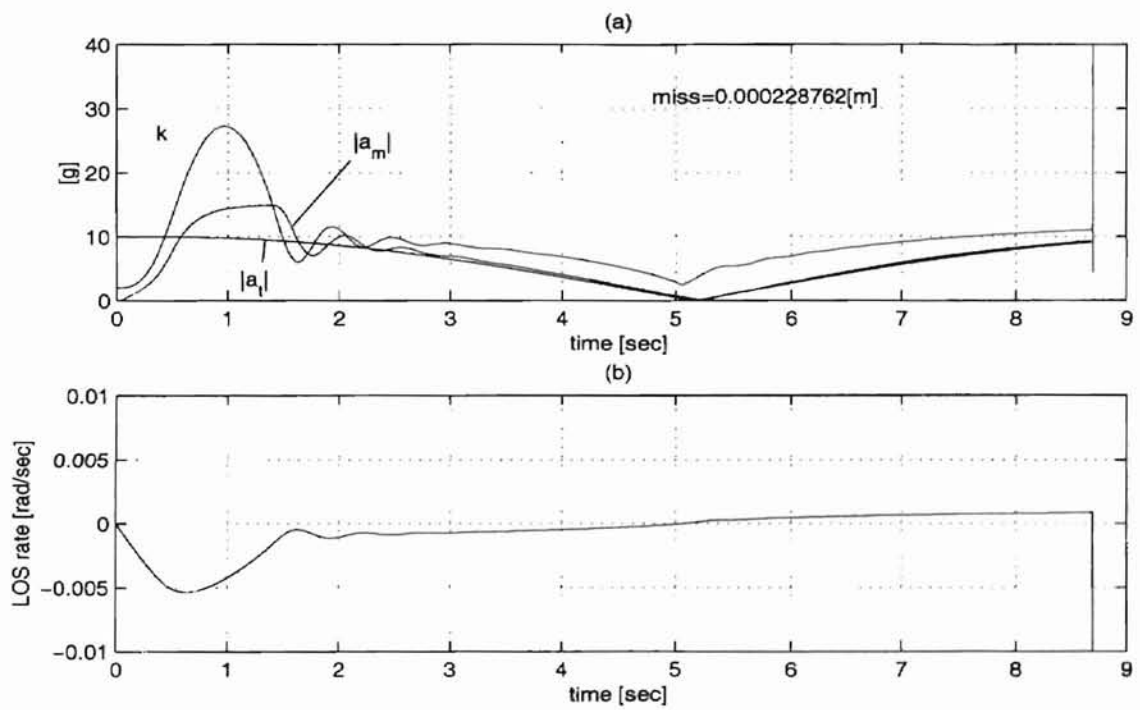


Figure 3.13: Control gain k without initial heading error (a) Acceleration (b) LOS rate (s)

3.2.2 Comparison of Guidance Laws

PNG, TOG, COG and SMG are compared in some important parameters in an effort to study their characteristics. Three types of basic target maneuvering (none, simple, and weaving) were selected to see the behavior of each guidance law for different target maneuver, and the results of these are plotted together for easy comparison. In Figure 3.14 non-maneuvering target is considered with $-20deg.$ of missile initial heading error. Figure 3.15 is about simple $10g$ target maneuver and Figure 3.16 is the result for a weaving target. Missile initial heading error is $10deg.$ for both simple and weaving targets.

A. Drawbacks of Proportional Navigation Guidance

It is generally known that PNG is not effective for high maneuvering targets and requires several times higher acceleration capability of the missile for successful interception. The reason can be found from the simulation results.

LOS rate converges to zero for the non-maneuvering target, but diverges with rapid increasing rate as the missile approaches for the $10g$ and weaving targets. In geometrical consideration, when there exists target movement normal to LOS, LOS change gets bigger as a missile approaches a target even when the amplitude of the target motion remains the same. Naturally as missile-target relative distance decreases, the control proportional to such LOS rate commands rising acceleration that, in some cases for high maneuvering target, goes beyond the practical limitation the missile can afford and causes miss distance as is seen in the simple $10g$ target maneuver case.

LOS rate is proportional to target maneuvering. Highly maneuverable target can generate rapid change of the LOS angle, specially about the missile is close to the target. To follow the LOS rate generated by the target maneuvering without

saturation, the missile is required to have more acceleration capability than the target.

B. Optimality of Nulling LOS Rate Strategy

It is pretty interesting to see TOG, COG and SMG show almost identical behavior in all the simulation results. Though missile accelerations generated by TOG and COG are chattering, their trend has a good agreement with that of SMG. Accelerations generated by TOG, COG and SMG follow target acceleration even though target acceleration estimation process was not included in those guidance laws. TOG and COG also try to null LOS rate. SMG was designed to zero LOS rate, but the control objective of TOG and COG is to eliminate relative distance along reference axes. This shows the optimality of nulling LOS rate strategy. Consider the collision course in Figure 2.4 whose optimality was stated in the basis of non-maneuvering target. Another interpretation may be possible from the collision triangle. By keeping constant LOS, target and missile travel the same amount of distance in the direction of normal to LOS which means they consume the same amount of acceleration in that direction. For a maneuvering target whose future behavior and eventual position is unknown, it is practically impossible for missile to travel less distance and hence consume less control effort than that of the target. The only virtually possible way for a missile to realize minimum time and minimum acceleration is to travel the same amount of distance and consume the same amount of acceleration that the target does. In that point of view, nulling LOS rate strategy is of optimal in both time and control effort even for maneuvering targets. SMG zeroes LOS rate effectively to acquire the time and control-effort optimality which results in its identical behavior with TOG and COG. The fundamental idea of PNG is to null LOS rate, but according to simulation results it cannot null LOS rate successfully for maneuvering targets, which is considered to place the behavior of PNG apart from the other guidance laws. Comparison of the elapsed time for the interception in Table 3.2 shows TOG, COG, and SMG

(miss distance[m]/elapsed time[sec])

	PNG	TOG	COG	SMG
Figure 3.14	0.0926/6.796	0.0083/6.794	0.0084/6.794	0.0057/6.794
Figure 3.15	9.3680/8.904	0.0415/8.843	0.0084/8.843	0.0219/8.844
Figure 3.16	0.9435/6.874	0.0540/6.854	0.0567/6.854	0.0875/6.854

Table 3.2: Comparison of guidance laws in miss distance and time

require less interception time than PNG.

C. Acceleration Generation

The type of acceleration generation is distinguished between PNG and optimal and sliding mode guidance. PNG generates smooth acceleration overall which, as the missile approaches the target, is increasing, up to the maximum limit for the high maneuvering target. TOG, COG and SMG command high acceleration at the beginning while correcting heading error, and follow the target acceleration. Based on the acceleration generation type, it can be estimated that rapid missile heading-direction change is requested at the beginning for TOG, COG and SMG, and at the final for PNG.

D. Acceleration Switching of Time-optimal Guidance

The simulation results seem to explain the reason of high acceleration switching in TOG. It was shown that TOG tries to null the rotational rate of LOS. Even when the LOS rate slightly is off zero, TOG pushes the LOS rate towards zero with maximum control efforts as defined in the bang-bang logic to excess the zero line to opposite side. Again TOG thrusts LOS rate across the zero line to the other side. Thus LOS rate switches between positive and negative values continuously and hence acceleration and final states estimation do the same continuously.

E. Performance Dependency on Time

Performance dependency of each guidance law on target maneuvering time is observed in Figure 3.17. In this simulation missile and target velocity vectors initially lie on LOS directing to each other with distance of $12,000m$, which requires 10 seconds for interception without target maneuvering. Then the target begins $10g$ maneuver at different time. One example of missile-target trajectory for the target starting maneuver at 1.5 sec. are given in Figure 3.17 (a). In Figure 3.17 (b), x -axis records the time when target starts its maneuver after the simulation starts and y -axis plots corresponding miss distance of each guidance laws. Actuator saturation and response delay are considered in this simulation. The result shows that TOG, COG and SMG have more stable performance against target maneuvering time than PNG does. This implies optimal and sliding mode guidance laws may not permit optimal target maneuver time that may exist in PNG [28].

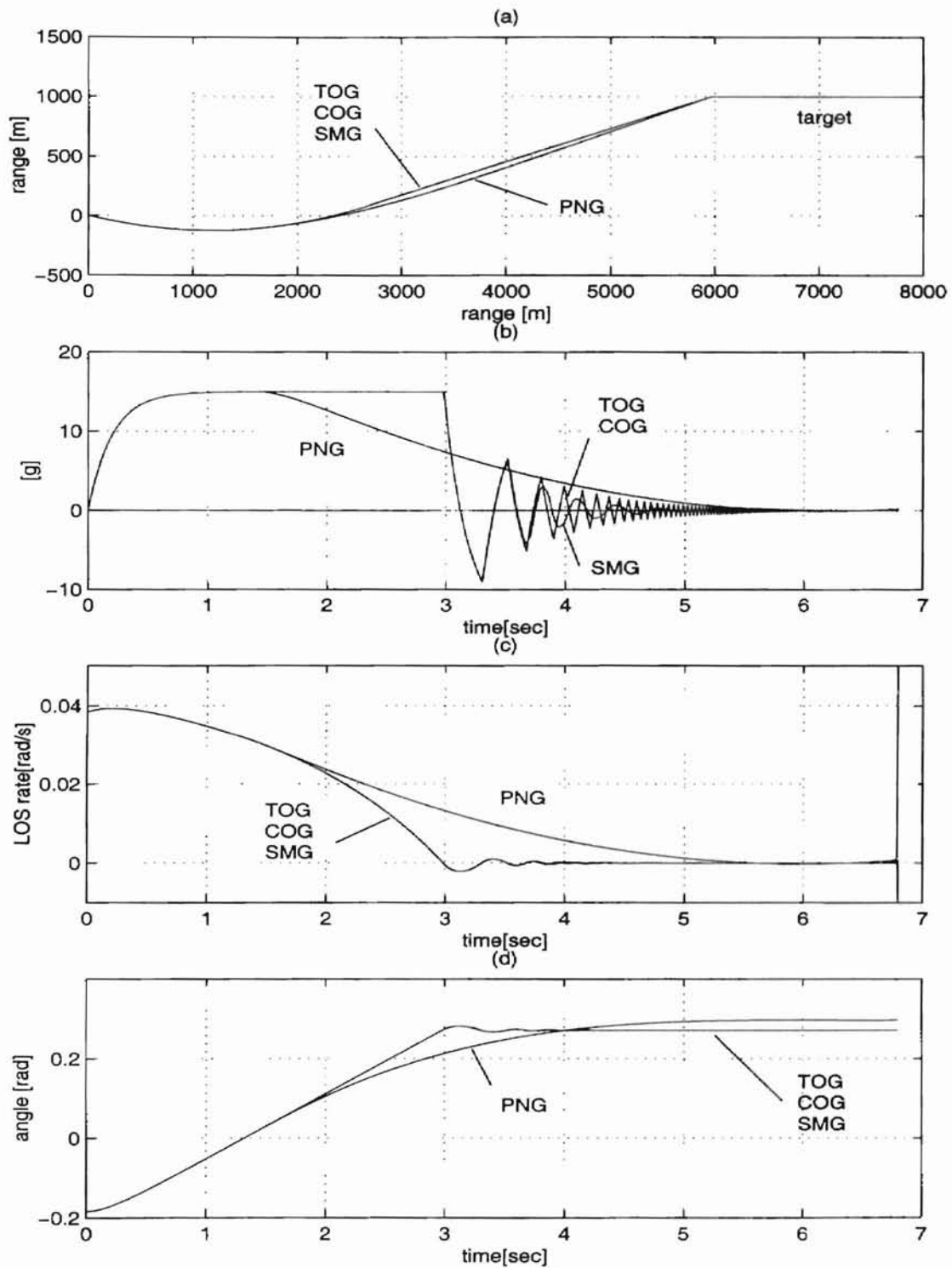


Figure 3.14: Comparison of guidance laws for a non-maneuvering target : (a) Missile-target engagement (b) Acceleration (c) LOS rate (d) Missile flight path angle and LOS angle

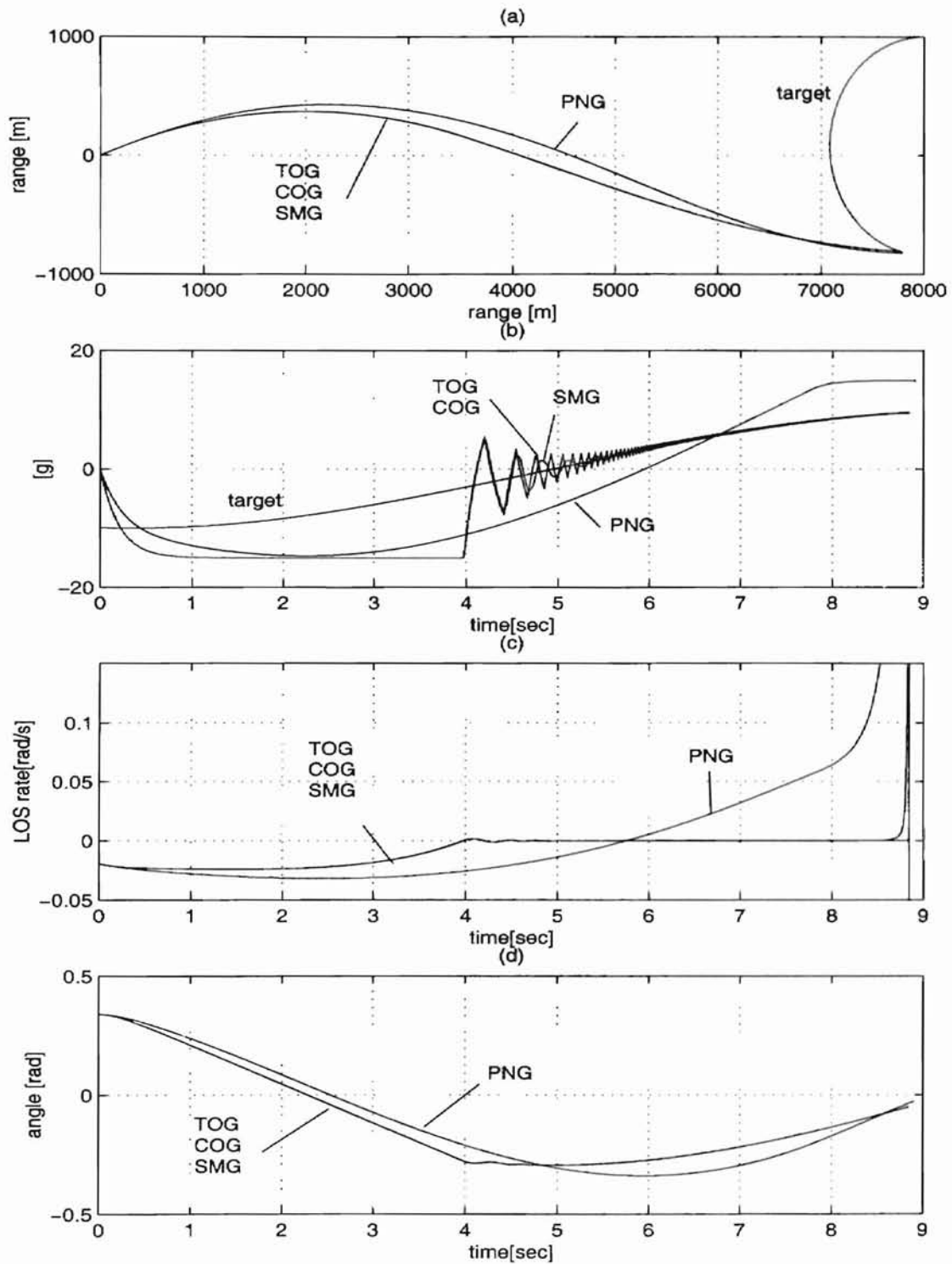


Figure 3.15: Comparison of guidance laws for a simple 10g maneuvering target : (a) Missile-target engagement (b) Acceleration (c) LOS rate (d) Missile flight path angle and LOS angle

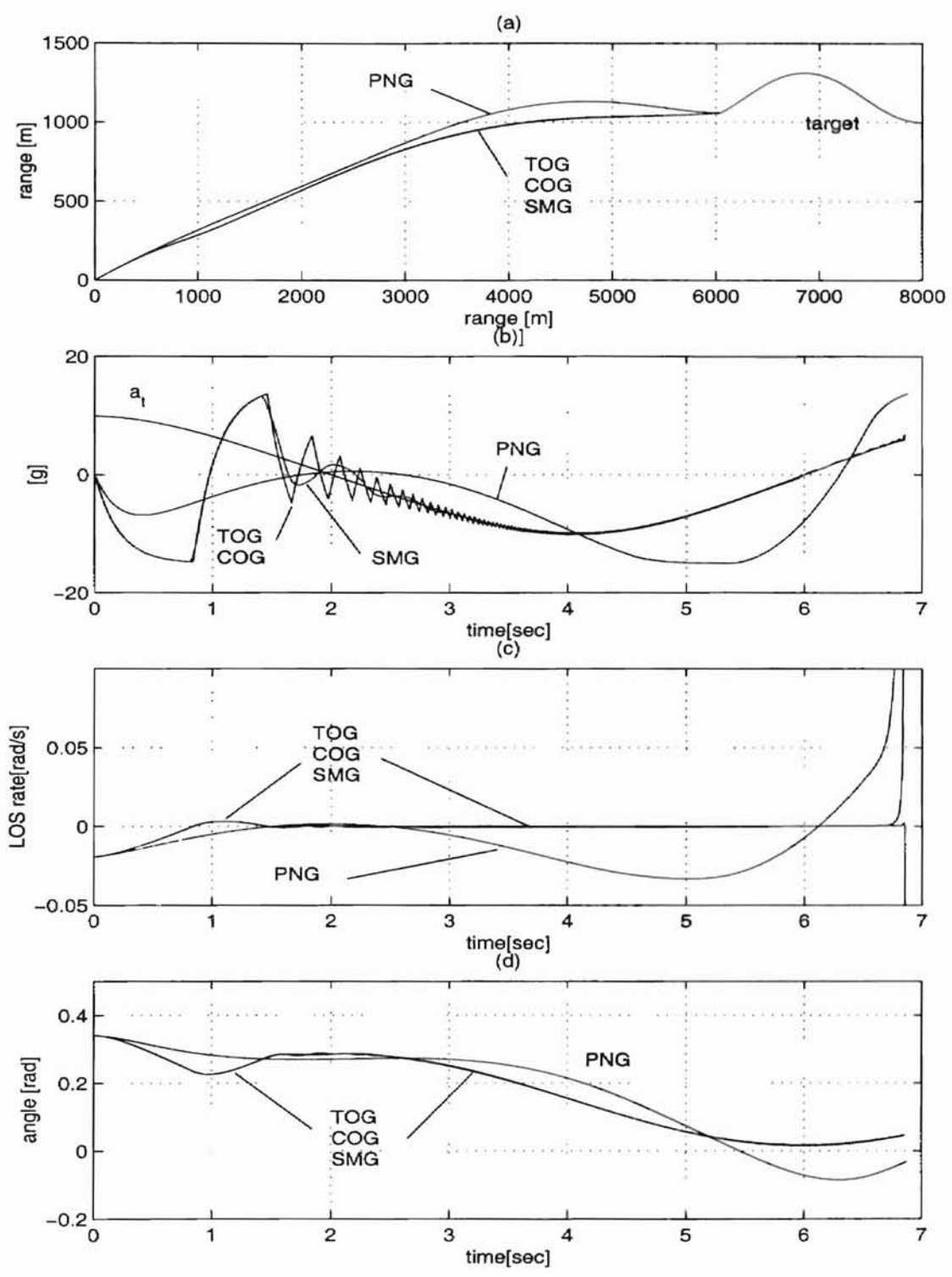


Figure 3.16: Comparison of guidance laws for a weaving target : (a) Missile-target engagement (b) Acceleration (c) LOS rate (d) Missile flight path angle and LOS angle

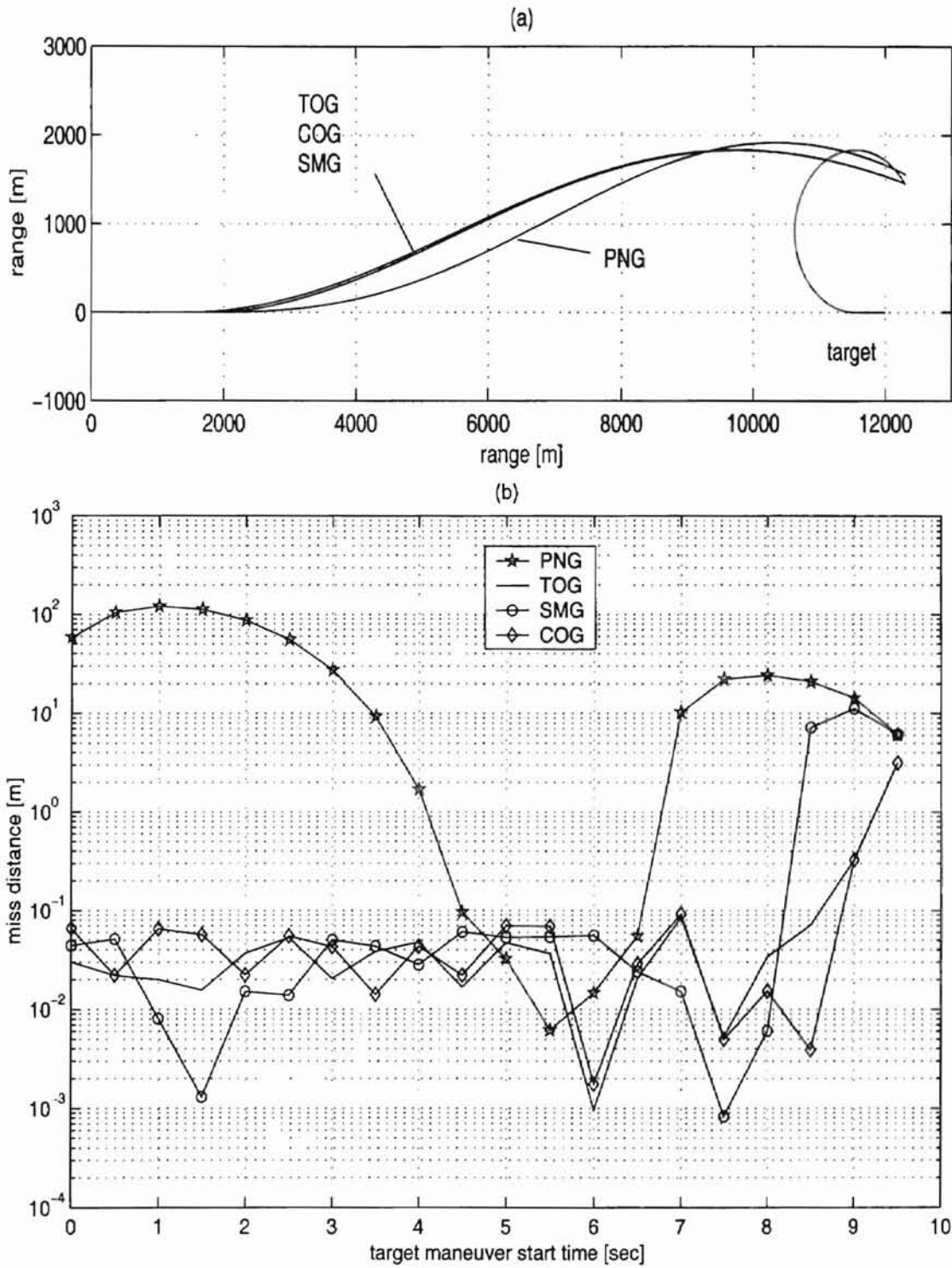


Figure 3.17: Miss distance to different target maneuver start time : (a) An example of missile-target engagement (b) Miss distance comparison

3.3 3D Simulation Results

Figure 3.18 gives a graphical demonstration of 3D engagement of each guidance laws along with its plane views, where the target initially directs to the missile for a while and then turns around to fly away, changing overall interception process from a head-on to a tail-chasing case. The θ plane view contains missile and target locations in θ plane at every instant and, as angle θ changes continuously, is actually not of plane trajectories. The ϕ plane view is of missile-target trajectory projected on ϕ plane. As is seen in 2D simulation, optimal and sliding mode guidance result in the identical missile trajectories.

Various factors affect miss distance such as missile-target relative position and direction at the final interception stage as well as target maneuvering type, which makes it difficult to decide one typical target maneuver model or two to compare the performance of guidance laws. To get more reliable results for various engagement situation, miss distances are computed statistically for a randomly maneuvering target whose acceleration is of uniformly distributed random numbers in between $\pm 10g$ with frequency of 0.5. In the evaluation of system performance for random inputs, the accuracy of the computation increases when large number of samples are involved. Considering trade-off between computation time and accuracy, 400 Monte Carlo simulations were performed. To make it more realistic, target acceleration is also assumed to have 1st order lag with time constant 0.2 sec.. An example of target acceleration is given in Figure 3.24. Noise effect is included in this 3D simulation. The noise is assumed Gaussian white noise with zero mean and $100m^2/s^2$ of standard deviation for range rate, and zero mean and $10^{-3}rad^2/s^2$ of standard deviation for LOS rate, unless noted.

The statistical results of miss distance are provided in Figure 3.19-3.23 and are

summarized in Table 3.3. Figure 3.19 compares miss distance where the target initially located at $(6000, 1000, 1000)[m]$. Acceleration ratio of missile to target and the ratio of elapsed time to target acceleration are compared as well as miss distance, where PNG used less acceleration at the cost of more miss distance. In other words PNG doesn't generate enough acceleration required for successful interception of targets. This again can be explained by basic control logic of PNG: proportional to LOS rate. PNG acceleration command increases as a missile approaches a target. About the final stage high acceleration is commanded that is cut-off by actuator saturation, which prohibits a PNG guided missile from following the command and causes less acceleration usage.

Figure 3.20 is the result when target initial location is increased to $(9000, 3000, 3000)[m]$, and shows the flying time doesn't change the performance trend.

Figure 3.21 compares guidance laws when target velocity is two times higher ($v_m = 400m/s$, $v_t = 800m/s$). Upon the faster target, interception is impossible in tail-chasing case. If the target maintains some high acceleration in one direction for a duration of time, then the target velocity vector could turn around to the opposite direction to establish tail-chasing case. To prevent this situation, target acceleration model is modified to switch between '+' and '-' at every frequency so that target maneuver is restricted to head-on case only.

Figure 3.22 and Figure 3.23 examine noise effect. In Figure 3.22 standard deviation of the noise associated with range rate is increased by ten-times to $1000m^2/s^2$, and in Figure 3.23 standard deviation of LOS rate noise is intensified by ten-times to $10^{-2}rad^2/s^2$. In both cases, TOG and COG cause more miss distance than SMG. It is considered that noise driven time-to-go and final states estimation error corrupts the performance of the optimal guidance.

For all the situation, optimal and sliding mode guidance demonstrate distinguished reliable interception performance over PNG.

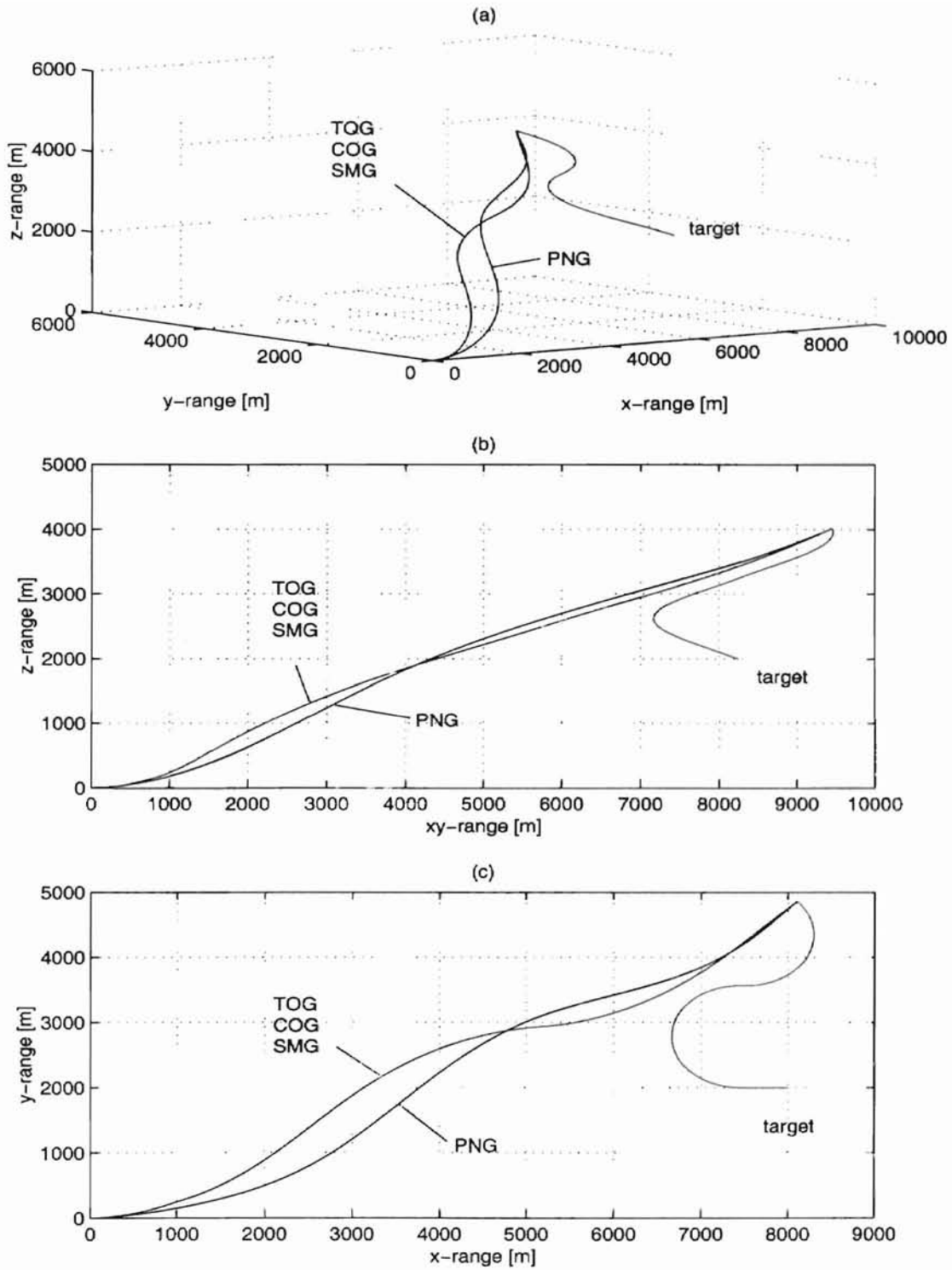


Figure 3.18: 3D missile-target engagement : (a) Missile-target engagement (b) θ plane view (c) ϕ plane view

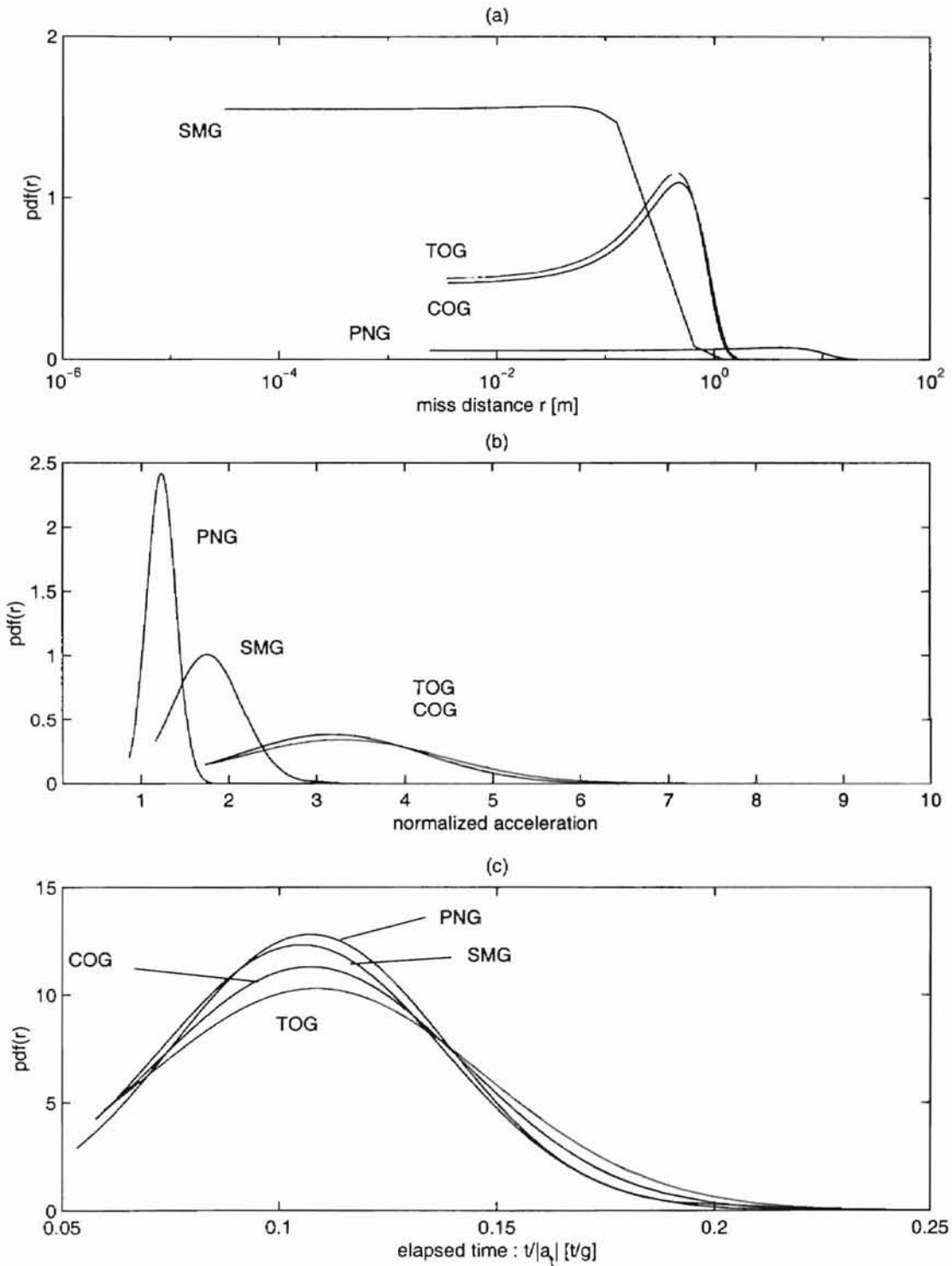


Figure 3.19: Statistical miss distance comparison 1: Initial distance (6000,1000,1000)
 (a) Miss distance (b) Missile acceleration usage (c) Elapsed time

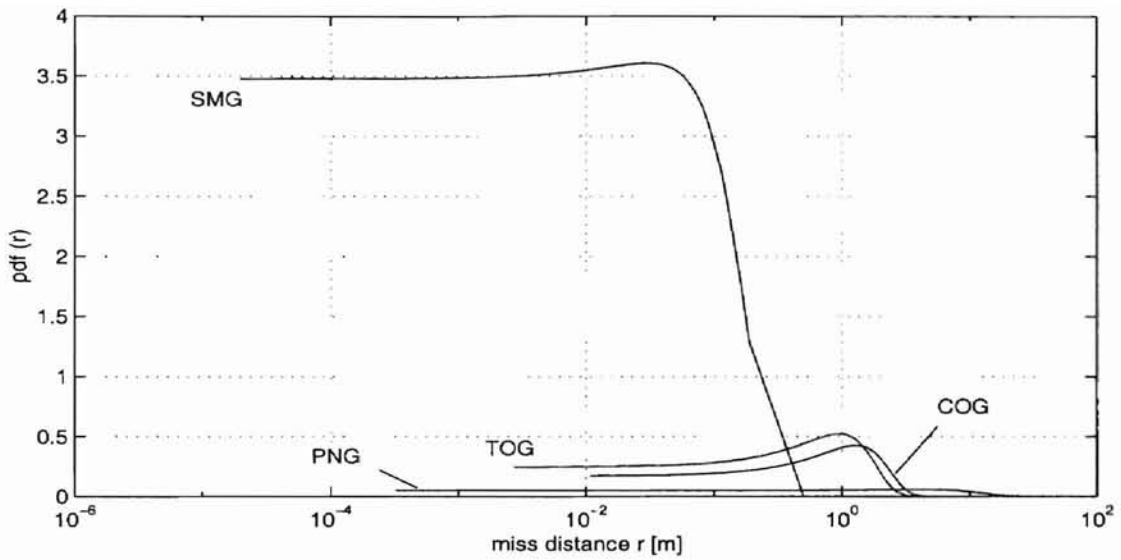


Figure 3.20: Statistical miss distance comparison 2: Initial distance (9000,3000,3000)

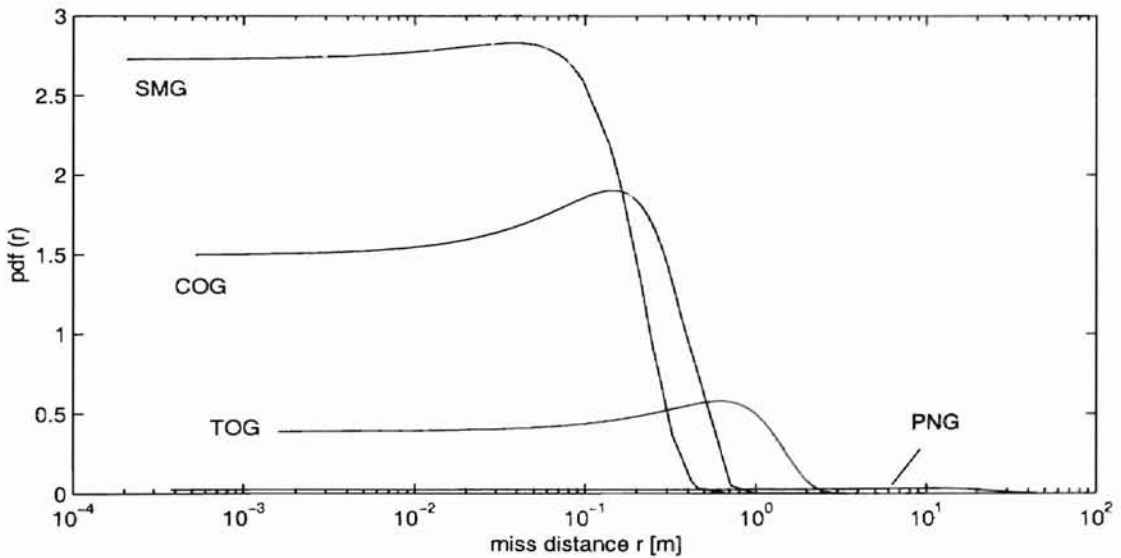


Figure 3.21: Statistical miss distance comparison 3: $v_m = 400\text{m/s}$ $v_t = 800\text{m/s}$, Initial distance (7000,0,0)

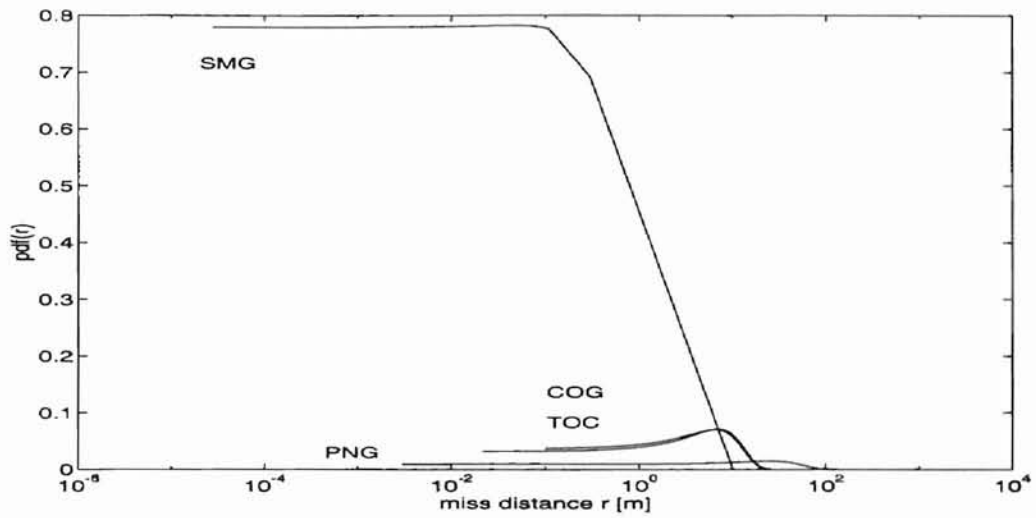


Figure 3.22: Statistical miss distance comparison 4: Initial distance (6000,1000,1000), range rate noise (0, 1000)

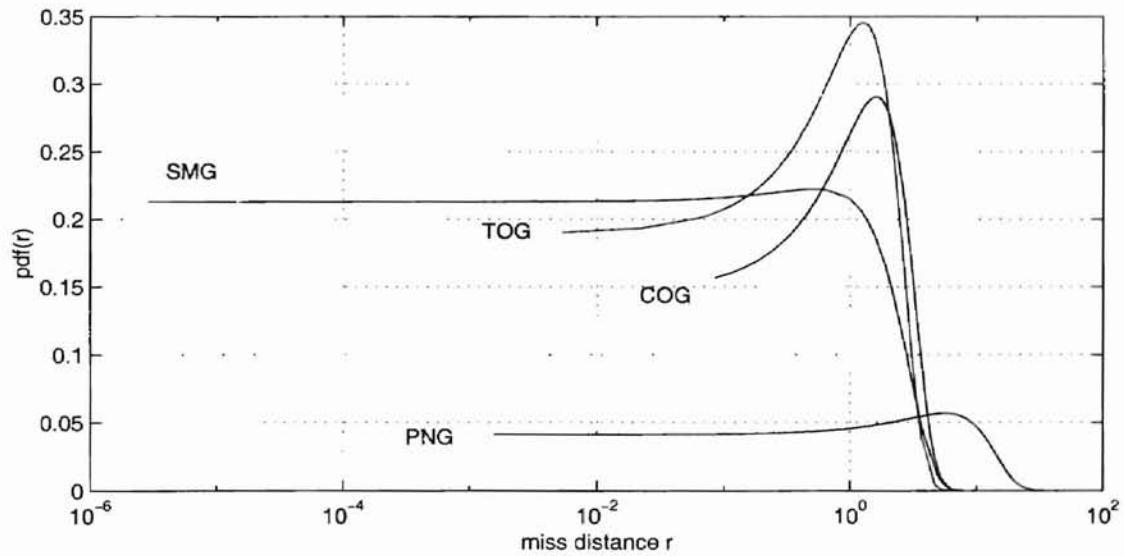


Figure 3.23: Statistical miss distance comparison 5: Initial distance (6000,1000,1000), LOS rate noise (0, 10^{-2})

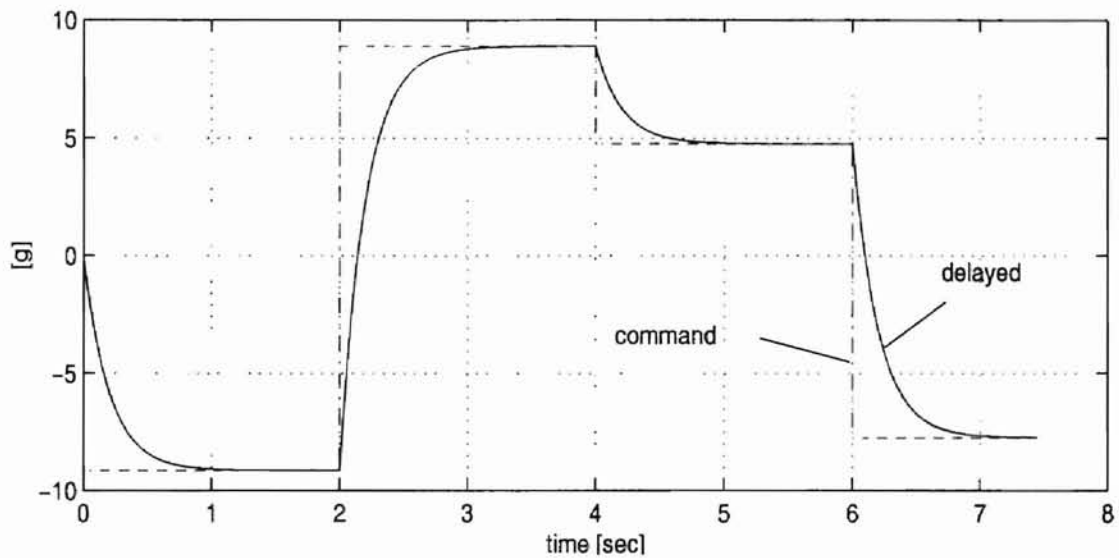


Figure 3.24: An example of random target acceleration

(mean , standard deviation) [m]

	PNG	TOG	COG	SMG	Remarks
Fig.3.19	(4.54,6.04)	(0.43,0.62)	(0.51,0.38)	(0.04,0.26)	
Fig.3.20	(4.09,6.96)	(0.95,0.76)	(1.28,0.94)	(0.03,0.11)	
Fig.3.21	(10.19,11.91)	(0.62,0.70)	(0.15,0.21)	(0.04,0.14)	$v_m < v_t$
Fig.3.22	(26.16,27.01)	(6.48,5.70)	(7.09,5.60)	(0.04,0.51)	\dot{r} (0,1000)
Fig.3.23	(5.64,7.01)	(1.27,1.16)	(1.61,1.37)	(0.53,1.80)	$\dot{L}OS(0, 10^{-2})$

Table 3.3: Summary of statistical miss distance

Chapter 4

Conclusion

Time-optimal, control-effort optimal and sliding mode guidance laws were constructed using three-dimensional nonlinear engagement model and compared with conventional PNG in characteristics and interception performance via numerical simulation. Simulation results demonstrated that optimal and sliding mode guidance laws are more effective in interception of highly maneuverable target than PNG, and they even have invariant interception performance against target maneuver type and time. The optimal and sliding mode guidance require more complicated controllers than PNG, but the required measurements are the same for all the guidance laws: range and range angle and those rate, and missile velocity and pitch and yaw angles.

Sliding mode guidance shows consistence performance for various target maneuvering and noise, and demonstrates its invariance towards disturbances. Because of the second derivative in the derivation of sliding mode control law, target acceleration inevitably appears in the equation - either explicitly or implicitly depends on the choice of engagement geometry. The simplest way is probably to insert an estimated upper bound of target acceleration into the equation, or an adaptation logic may be necessary in the sliding mode guidance law.

Time-to-go estimation is necessary in optimal guidance because of the time-integral in optimization process. The optimal guidance laws proposed in this paper

requires final states estimation as well as time-to-go estimation. Estimation error for those quantities can severely degrade the guidance performance, but it was observed that, by the simplest algorithm, the estimation nicely converges and achieves excellent performance.

The high switching of acceleration command in the time-optimal guidance law may be a problem in its practical implementation. It was shown that by increasing missile dynamics time constant the acceleration switching can be attenuated without severe loss of performance. Yet stiff transition of the missile acceleration still exist in both optimal guidance laws because of instantaneous control switching between two maximum values. Near-minimum-time optimal [14] concept may be worth to be investigated to minimize acceleration command rate for smooth control.

Guidance problem resembles shooting problem. Given missile velocity has superiority over target velocity, relative distance between missile and target naturally decrease whether it is head-on case or tail-chasing case. Then control interest is left only on lateral deviation of missile from target. In that point of view, nulling LOS rate strategy structures powerful guidance technique in that it set a criterion (i.e. LOS) and control the lateral motion of missile from the criterion, which, as observed in this research, eventually leads time-control-effort optimal guidance regardless of the type of target maneuvering. PNG cannot effectively zero LOS rate for high maneuverable targets. Modern control logic, optimal and sliding mode, is examined to provide more systematic framework for this purpose.

Bibliography

- [1] Fred P. Adler. Missile guidance by three-dimensional proportional navigation. *Journal of Applied Physics*, Vol 27, No 5, pp 500–507, 1956.
- [2] K.R. Babu, I.G. Sarma, and K.N. Swamy. Switched bias proportional navigation for homing guidance against highly maneuvering targets. *J.Guidance, Control and Dynamics*, Vol 17, No 6, pp 1357–1363, 1994.
- [3] K.R. Babu, I.G. Sarma, and K.N. Swamy. Two robust homing missile guidance laws based on sliding mode control theory. *Proceedings of NAECON, Dayton, OH*, pp 540–547, 1994.
- [4] D.G. Benshabat and A. Bar-Gill. Robust command-to-line-of-sight guidance via variable-structure control. *IEEE Transactions on Control Systems Technology*, Vol 3, No 3, pp 356–361, 1995.
- [5] S.D. Brierley and R. Longchamp. Application of sliding-mode control to air-air interception problem. *IEEE Transactions on Aerospace and Electronic Systems*, Vol 26, No 2, pp 306–324, 1990.
- [6] V.H.L. Cheng and N.K. Gupta. Advanced midcourse guidance for air-to-air missiles. *J. Guidance*, Vol 9, No 2, pp 135–142, 1986.
- [7] James R. Cloutier, Johnny H. Evers, and Joseph J. Feeley. Assessment of air-to-air missile guidance and control technology. *IEEE Control Systems Magazine*, Vol 9, pp 27–34, 1989.

- [8] R.A. Decarlo, S.H. Zak, and G.P. Matthews. Variable structure control of non-linear multivariable systems: A tutorial. *Proceedings of the IEEE*, Vol 76, No 3, pp 212–232, 1988.
- [9] Takayuki Furuta and Ken Tomiyama. Two adaptive robust sliding mode controllers for robot manipulators. *JSME International Journal*, Vol 40, No 1, pp 104–111, 1997.
- [10] Donald T. Greenwood. *Principle of Dynamics*. Prentice Hall, 1965.
- [11] R.D. Hartman, F.H.Lutze, and E.M. Cliff. Time-optimal maneuver guidance design with sensor line of sight constraint. *SPIE Sensors and Sensor Systems for Guidance and Navigation*, Vol 1478, pp 64–75, 1991.
- [12] David G. Hull, Jerry J. Radke, and Rodney E. Mack. Time-to-go prediction for homing missiles based on minimum-time intercepts. *J.Guidance*, Vol 14, No 5, pp 865–871, 1991.
- [13] John Y. Hung, Weibing Gao, and James C. Hung. Variable structure control: A survey. *IEEE Transactions on Industrial Electronics*, Vol 40, No 1, pp 2–20, 1993.
- [14] John E. Hurtado and John L. Junkins. Optimal near-minimum-time control. *J.Guidance, Control and Dynamics*, Vol 21, No 1, pp 172–174, 1998.
- [15] Emil J. Eichblatt Jr., editor. *Test and Evaluation of the Tactical Missile*, volume 119 of *Progress in Astronautics and Aeronautics*. AIAA, 1989. Chapt. 1, 2.
- [16] Donald E. Kirk. *Optimal Control Theory*. Prentice Hall, 1970.
- [17] Eliezer Kreindler. Optimality of proportional navigation. *AIAA Journal*, Vol 11, No 6, pp 878–880, 1973.

- [18] S.A. Murtaugh and H.E. Criel. Fundamentals of proportional navigation. *IEEE Spectrum*, Vol 3, No 12, pp 75–85, 1966.
- [19] H.L. Pastrick, S.M. Seltzer, and M.E. Warren. Guidance laws for short-range tactical missiles. *J.Guidance and Control*, Vol 4, No 2, pp 98–108, 1981.
- [20] A.I.A. Salama and M.H. Hamza. Minimum time three dimensional interception. *Acta Astronautica*, Vol 5, pp 515–522, 1978.
- [21] G.M. Siouris and A.P. Leros. Minimum-time intercept guidance for tactical missiles. *Control-Theory and Advanced Technology*, Vol 4, No 2, pp 251–263, 1988.
- [22] J.-J. E. Slotine. *Applied Nonlinear Control*. Prentice Hall, 1991.
- [23] T.Y. Song and S.J. Shin. Time-optimal impact angle control for vertical plane engagement. *IEEE Transactions on Aerospace and Electronic Systems*, Vol 35, No 2, pp 738–742, 1999.
- [24] V.I. Utkin. Variable structure systems with sliding modes. *IEEE Transactions on Automatic Control*, Vol AC-22, No 2, pp 212–222, 1977.
- [25] V.I. Utkin. Discontinuous control system: State of art in theory and application. *IFAC 10th Triennial World Congress, Munich, FRG*, pp 25–44, 1987.
- [26] K.D. Yong, V.I. Utkin, and Umit Ozguner. A control engineer's guide to sliding mode control. *IEEE Transactions on Control Systems Technology*, Vol 7, No 3, pp 328–342, 1999.
- [27] D.S. Yoo and M.J. Chung. A variable structure control with simple adaptation laws for upper bounds on the norm of the uncertainties. *IEEE Transactions on Automatic Control*, Vol 37, No 6, pp 860–864, 1992.

- [28] Paul Zarchan. *Tactical and Strategic Missile Guidance*, volume 176 of *Progress in Astronautics and Aeronautics*. AIAA, 3rd edition, 1997.
- [29] Di Zhou, Chundi Mu, Qiang Ling, and Wenli Xu. Optimal sliding-mode guidance of a homing-missile. *Proceedings of the 38th Conference on Decision and Control, Phoenix, Arizona, USA*, pp 5131–5136, 1999.
- [30] Di Zhou, Chundi Mu, and Wenli Xu. Adaptive sliding-mode guidance of a homing missile. *J. Guidance, Control and Dynamics*, Vol 22, No 4, pp 589–594, 1999.

Appendix A

Simulation Program

- Schematic Diagram of Missile Guidance
- PN Guidance Simulation Program
- Optimal Guidance Simulation Program
- Sliding Mode Guidance Simulation Program

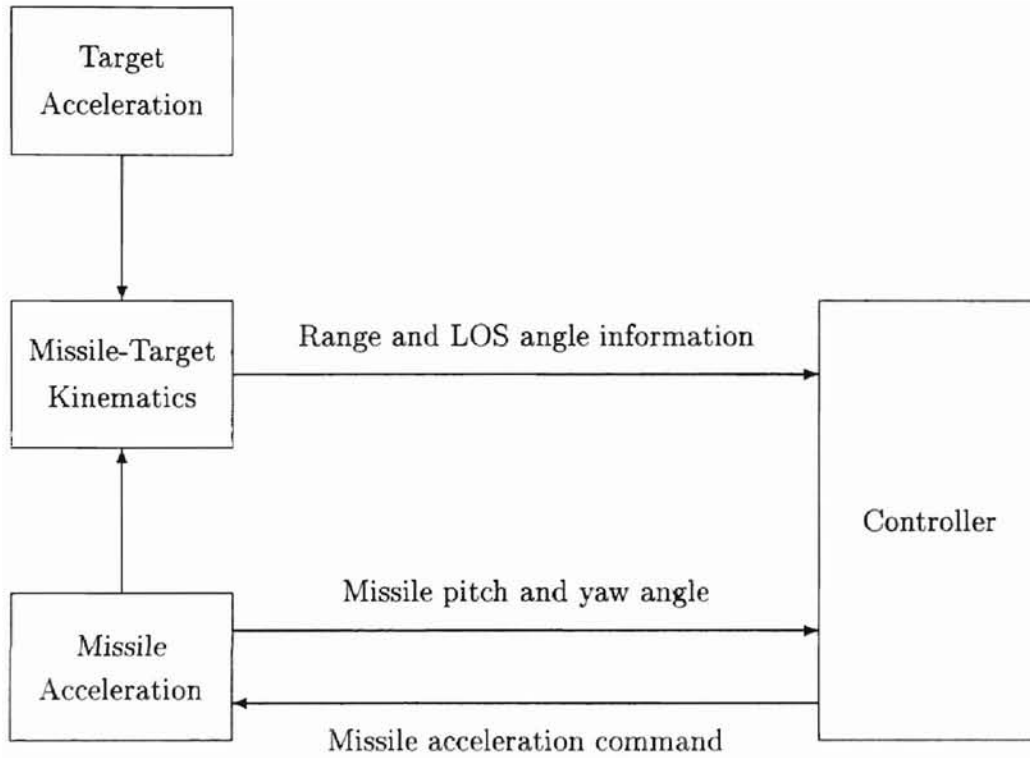


Figure A.1: Missile Guidance Schematic Diagram

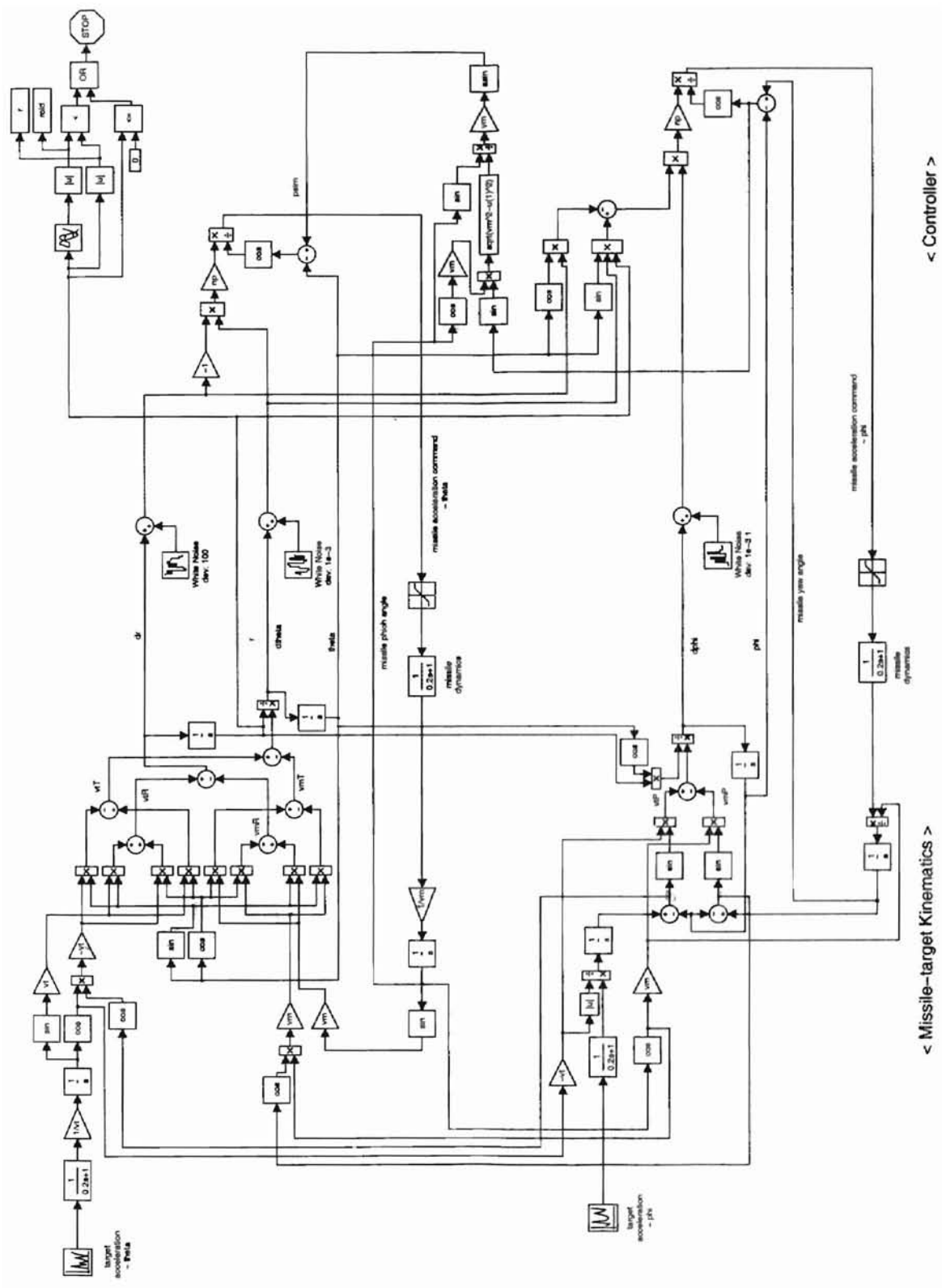


Figure A.2: PN Guidance Simulation Program

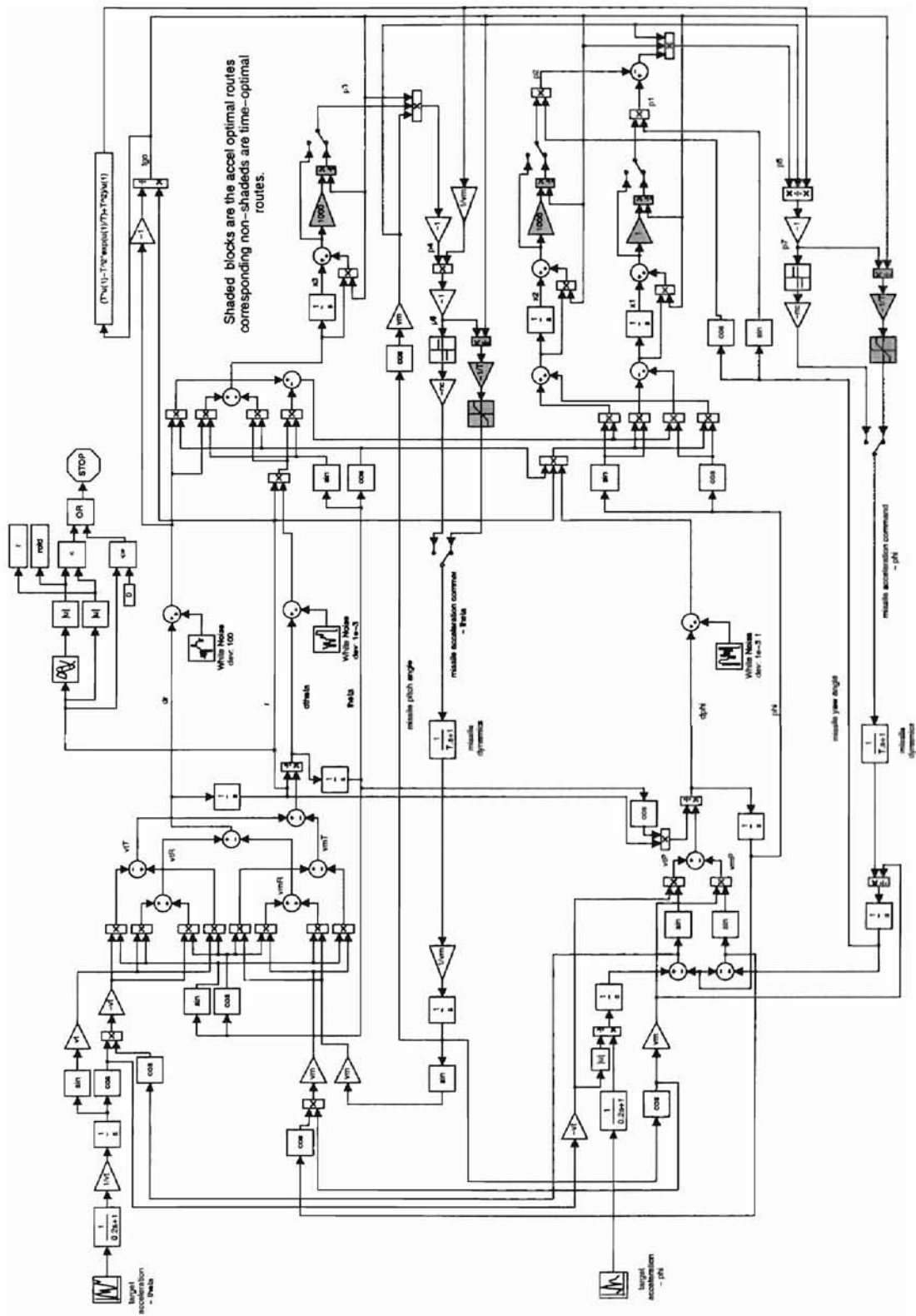


Figure A.3: Optimal Guidance Simulation Program

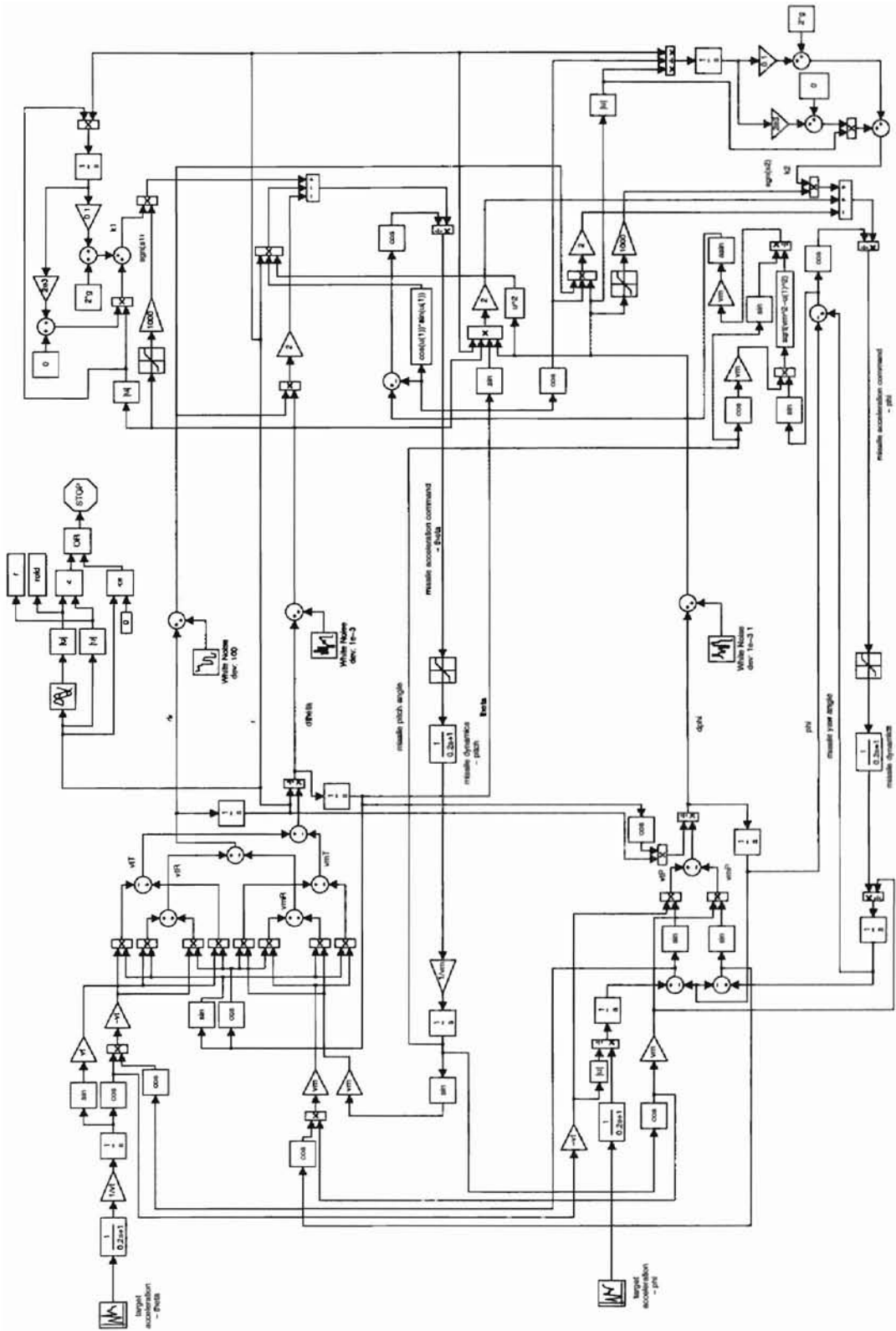


Figure A.4: Sliding Mode Guidance Simulation Program

VITA

Jae Hong Seo

Candidate for the Degree of
Master of Science

Thesis: A STUDY ON OPTIMAL AND SLIDING MODE GUIDANCE FOR AN
INTERCEPTION PROBLEM

Major Field: Mechanical Engineering

Biographical:

Education: Received Bachelor of Science degree in Mechanical Engineering from Inha University, Inchon, Korea in February 1996. Completed the requirements for the Master of Science degree with a major in Mechanical Engineering at Oklahoma State University in December 2000.

Experience: Employed by Kia Motors Inc. in Korea as an engineer to August 1998.